# Instrumentation and analysis strategies to search for particle precipitation from space


Livio Conti

*On behalf of the Italian collaboration to the **CSES** project*

UTIU
UNIVERSITÀ TELEMATICA INTERNAZIONALE UNINETTUNO

conti.livio@gmail.com

# Talk overview

Instrumentation and analysis strategies to search for particle precipitation from space

VOLTA
Electric Field Detector
for the CSES satellite

# SAMPEX-PET mission and database

## Main characteristics of the SAMPEX/PET mission:

| | |
|---|---|
| Orbit altitude: | 520÷670 km |
| Orbit inclination: | 82° |
| PET Pointing modes: | ORR; MORR; 1 RPM (see text) |

## PET channel Level-2 data used for this study

| Particles | Energy (MeV) | Geometric factor ($cm^2 sr$) | Channel |
|---|---|---|---|
| Protons | 28÷60 | 1.5 | PHI |
| Protons | 19÷28 | 1.65 | PLE |
| Electrons | 2÷6 | 1.65 | ELO |
| Electrons | 4÷15 | 1.5 | EHI |
| Electrons | 4÷30 | - | EWG |
| Protons | > 60 | 0.4 | RNG |
| Electrons | > 15 | | |
| Protons | > 85 | 0.25 | PEN |
| Electrons | > 30 | | |

# SAMPEX Pointing Modes

**SAMPEX/PET has operated with three different pointing programs:**

- **ORR** (original **O**rbit **R**ate **R**otation)
- **MORR** (**M**odified **O**rbit **R**ate **R**otation)
- **1 RPM** (**1 R**otation **P**er **M**inute)

✓During the ORR pointing mode the **PET yaw axis is substantially radial to the Earth**. So, PET may detect particles with pitch angle in a wide range and, in particular, also in the **loss cone** (precipitating particles) or near to it.

✓On the contrary, in the MORR mode the detector yaw axis is fundamentally **perpendicular to the geomagnetic field lines**, since it was implemented mainly to study particles with pitch angle near 90° (**trapped particles**). Measurements for $\alpha_{PET}$ values far from 90° are performed in periods during which PET yaw axis is parallel to the geomagnetic field (B), when B > 0.3 G, and perpendicular to it, when B < 0.3 G.

✓Finally, in the 1 RPM mode the $\alpha_{PET}$ distribution is flat since **the PET yaw axis, rotating continuously at 1 RPM**, allows the particle detection at **any pitch angle value**.

# Particle Burst definition

- **Observations:**

PBs are particle fluxes characterized by an **anomalously sharp increase and time duration of a few ten seconds**. In a sequence of CRs (each one having a duration of 30 seconds) we observe a PB as an increase in the number of detected particles.

- **Duration:**

The duration of this time series of data is relatively short, since **it only consists of several CRs**. The 30s temporal resolution of Level-2 PET-data does not allow characteristic PB events to be individually observed. Then, only an anomalous deviation from the statistical distribution of the 30s integrated CRs can be identified.

- **Parameters:**

These PB events are defined beginning from CRs detected at known **L-shell** and $\alpha_{PET}$ **values**.

# From the Counting Rates to the Particle Bursts

## Construction of the *"Background matrix"*

- **L-shell and B** values for each CR detection position are **calculated by the IGRF**.
- Analysed L-shell interval: **$1.0 \leq$ L-shell $\leq 1.8$**
- **Background matrix:** $0° \leq \alpha_{PET} \leq 180°$ (step = 15°) **&** $1 \leq$ L-shell $\leq 1.8$ (8 steps of 0.1)

## CRs Poissonian selection creteria → PBs definition

✓ For each cell of the $\{L,\alpha_{PET}\}$ matrix, **the CR distribution is the reference background** for estimating PBs.

✓ **CRs have a Poissonian distribution** for each $\{L,\alpha_{PET}\}$ matrix cell.

✓ We define as PBs those counting rates which:

- assume **values greater than those of the relative $\{L,\alpha_{PET}\}$ background matrix**

**&**

- **probability to be a Poisson fluctuation is less than < 0.01**.

# Particle Bursts selection criteria

## Constraints:

- The **<u>lower boundary of the inner radiation belt</u>** (and in particular the SAA region) has been **determined yearly by the IGRF**

$\Downarrow$

**Exclusion of stably trapped particles** $\Rightarrow$ PBs are constituted by particle precipitating fluxes **!!**

- The **SAA region has been excluded** from this study.

- In order to reduce ionospheric and magnetospheric contamination from non-seismic sources, we use only data collected:

  - during periods characterized by a geomagnetic index value $\mathbf{A_P < 20}$
  - in absence of ionospheric disturbances **(SID=0)**.

# Particle Burst Catalogue

- Particle Burst definition:
  - ✓CRs = particle flux measurements every **30 seconds**
  - ✓CR background matrix $\{L, \alpha_{IDP}\}$:
  - ✓ **$1 \leq$ L-shell $\leq 1.8$ (step=0.1)**
  - ✓ **$60° \leq \alpha_{IDP} \leq 120°$ (step = 15°)**
  - ✓Poissonian cut $p < 0.01$
  - ✓No measurements in the SAA reagion
  - ✓$A_p < 20$ & SID = 0

- **PBEHI** & **PBELO** catalogues for the SAMPEX pointing mode periods:

| Pointing mode | Period (MM/DD/YY) | # "good days" | # CR | # CR per day | # PBEHI | # PBELO |
|---|---|---|---|---|---|---|
| ORR | 01/24/93÷05/26/94 | 247 | 211603 | 857 | 1734 | 1259 |
| MORR (1) | 05/27/94÷05/07/96 | 691 | 373976 | 541 | 3957 | 1848 |
| 1 RPM | 05/08/96÷05/06/98 | 677 | 195187 | 288 | 1253 | 485 |
| MORR (2) | 05/07/98÷12/16/99 | 543 | 179457 | 330 | 1628 | 698 |

Reported daily data have been collected with **optimal device working conditions** (here referred to as "**good days**") and detected with good quality flag according with the SAMPEX weekly instrument status report.

# SAMPEX measurements for different pointing modes

Geographic distributions of CRs

CRs distributions vs *L-shell*

CRs distributions vs $\alpha_{PET}$

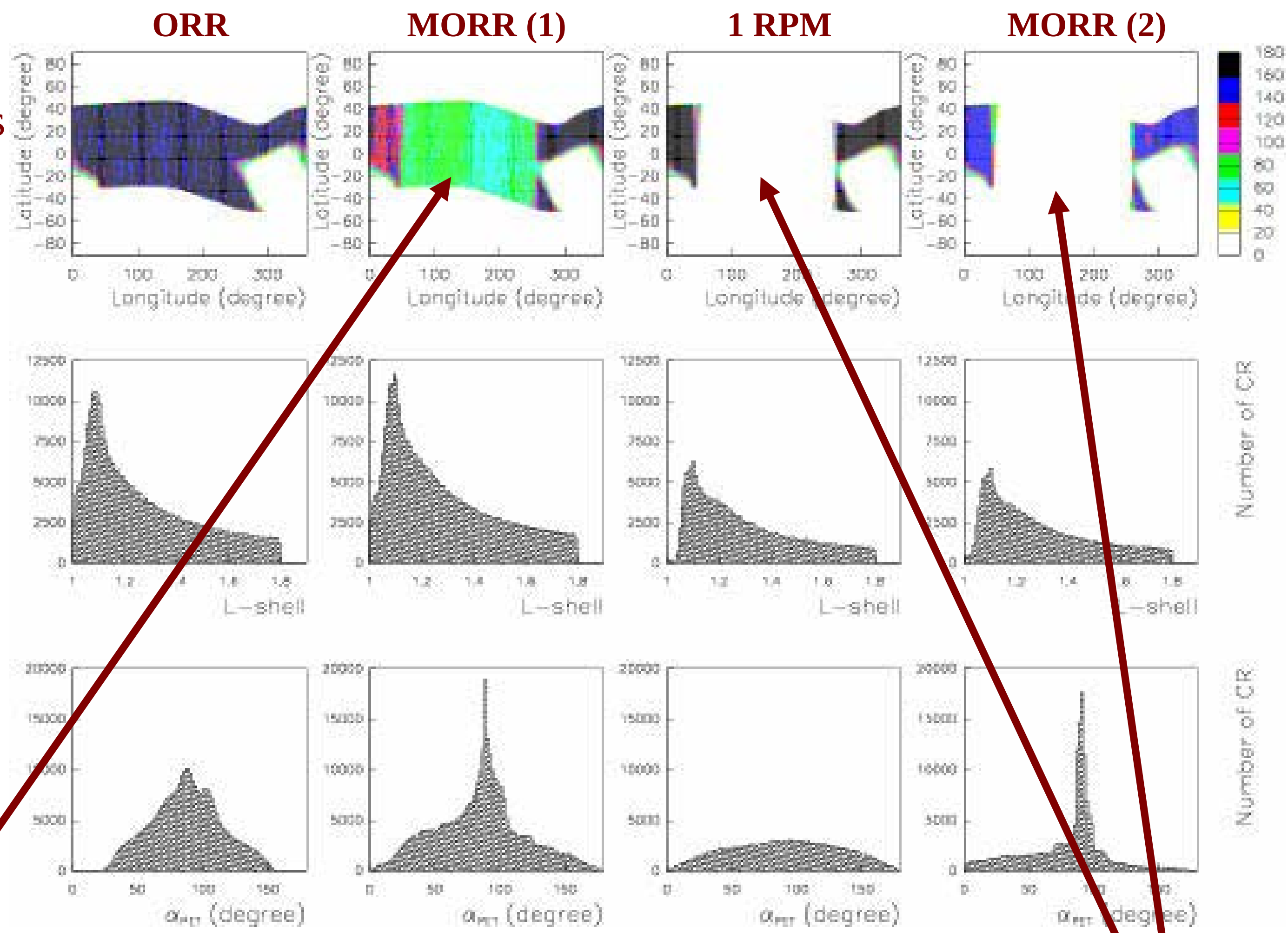


- During the MORR (1) mode there is a non-homogeneous CRs geographical distribution due to **scanty PET measurements in the longitude interval [50°-270°]**.
- PET measurements are further reduced in this longitudinal interval during the 1RPM and MORR(2) pointing programs.
- The 4 panels in the bottom confirm that the $\alpha_{PET}$ distribution is pointing program dependent.

# Geographic PBs distributions

**PBEHI**

**PBELO**

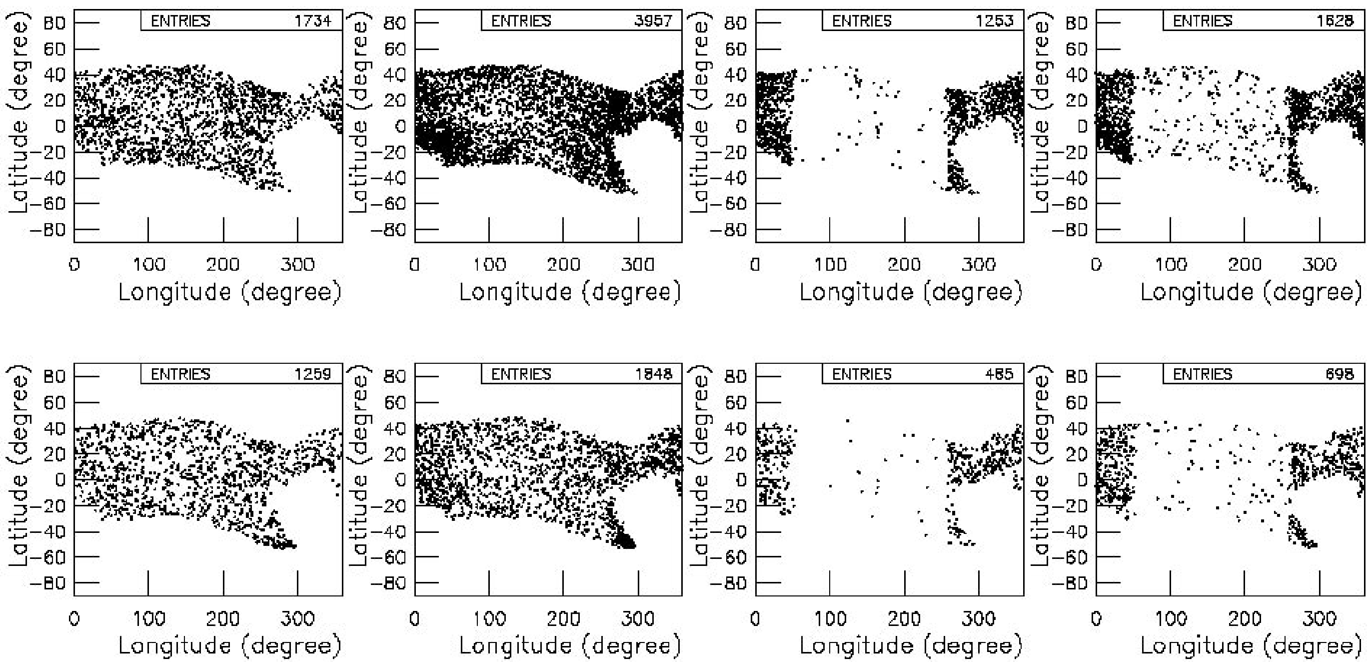


ORR MORR (1) 1 RPM MORR (2)

Geographic distributions of **PBEHI** (top) & **PBELO** (bottom) data in the $1.0 < L < 1.8$ interval for the 4 pointing modes.

# Earthquakes catalogue

**Earthquake selection (USGS catalogue):**

- **$M \geq 5.0$**
- **hypocentral depth $\leq$ 100 km**

**Seismic EME & particle interaction altitude:**

$$100 \text{ km} \leq Z_{EME} \leq 1200 \text{ km}$$

✂ **Earthquake, $L_{EME}$ = L-shell of the interaction zone between trapped particles & preseismic EME**

$$L_{EME} = L\Big|_{Z_{EME} = 400 \text{ km}}$$

# Selection criteria for the EQs and PBs populations to be correlated

| EQ event selection | PB event definition |
|---|---|
| $M \geq 5.0$<br>Hypocentral depth $h < 100km$<br><br>$L_{EME} \sim L_{z=400km}$ | CRs = particle flux measurements integrated over 30s<br>CR daily background matrix $\{L, \alpha_{PET}\}$:<br>$1.0 \leq L_{PB} \leq 1.8$ ($L$-step $= 0.1$)<br>$0° \leq \alpha_{PET} \leq 180°$ ($\alpha_{PET}$-step $= 15°$)<br>Poissonian cut: $p < 0.01$<br>No measurements in the SAA region<br>$A_p < 20$<br>SID = 0 |

***EQ-PB correlation***

$\Delta L = L_{EME} - L_{PB} < 0.1$

$\Delta T_{MAX} = (T_{EQ} - T_{PB})_{MAX} = \pm 3$ days

# SAMPEX: $\Delta T_{EQ\text{-}PB}$ correlations between PBs and Eqs

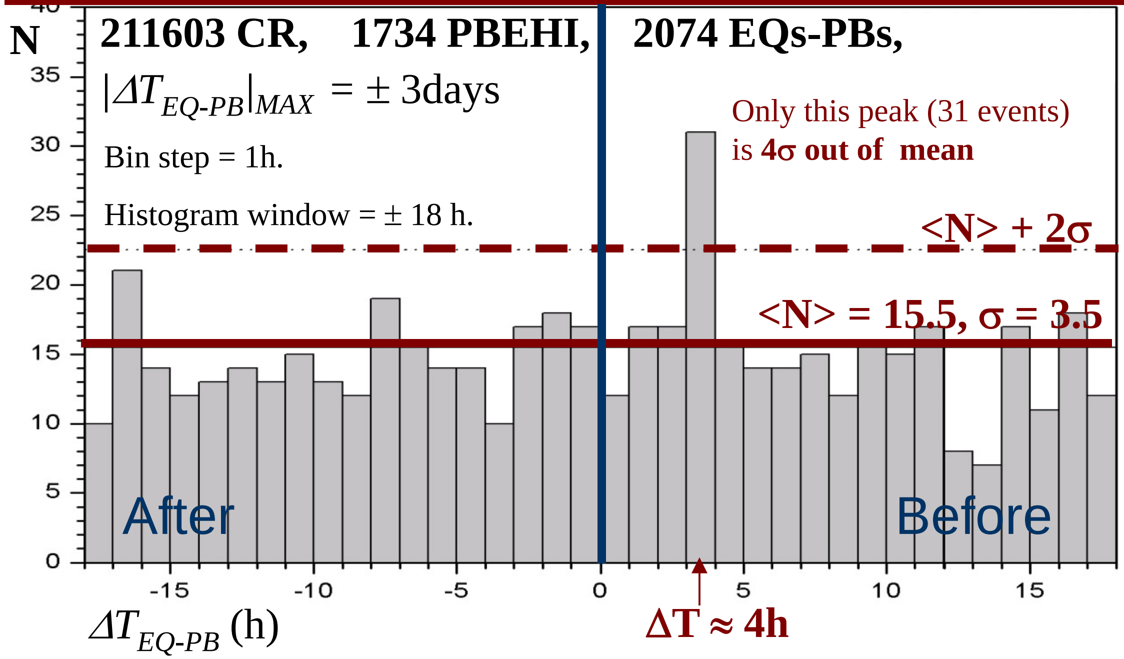


## ORR mode

- The existence of a ΔT > 0 peak suggests that **PB events statistically precede EQs** occurrence.
- ΔT maximum positive peak has been observed:
  - only when considering **PBEHI** data obtained during the **ORR** mode
  - **Not** maximum positive **peak** is found **for PBELO** data.

## Improvement of the $\Delta T_{EQ\text{-}PB}$ correlations with αPET cut

An increase of the peak $\Delta T_{EQ\text{-}PB}$ statistical significance in the ORR histogram is obtained by excluding data of charged particles with $\alpha_{PET} \approx 90^o$ (trapped particles).

Histogram is obtained by **excluding** $\alpha_{PET}$ range:

$$70^o < \alpha_{PET} < 110^o$$

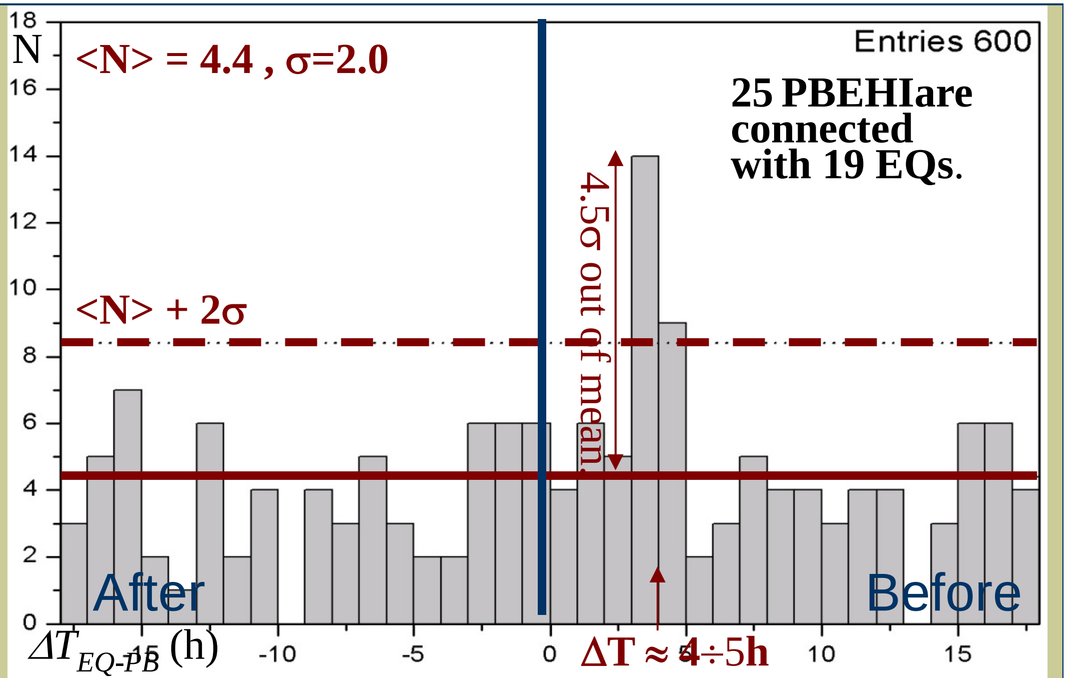

# Dependence of the $\Delta T_{EQ\text{-}PB}$ correlation on: the particles energy & the PET yaw axis orientation

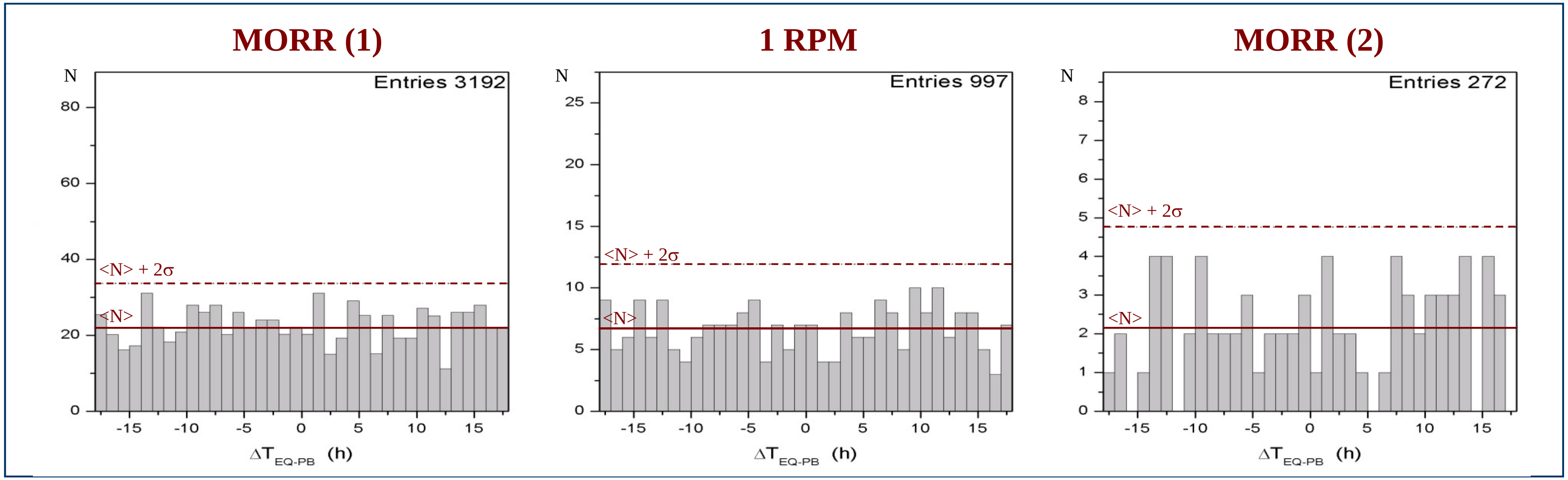


- ✓ **No correlation** is obtained (that is, no relevant peak is observed) with PBEHI data collected in the other **MORR(1)**, **1RPM**, and **MORR(2)** pointing periods
- ✓ **No correlation** is obtained in the 4 pointing mode periods with **PBELO** data.

  - The good correlation obtained only with ORR PBEHI suggest a **dependence from the particle energy** and confirms results reported in literature.
  - Our study results have demonstrated also a dependence of the $\Delta T_{EQ\text{-}PB}$ correlation on the **PET yaw axis orientation**

# Correlations between EQ & ps: $\Delta T_{EQ\text{-}PB}$ distributions

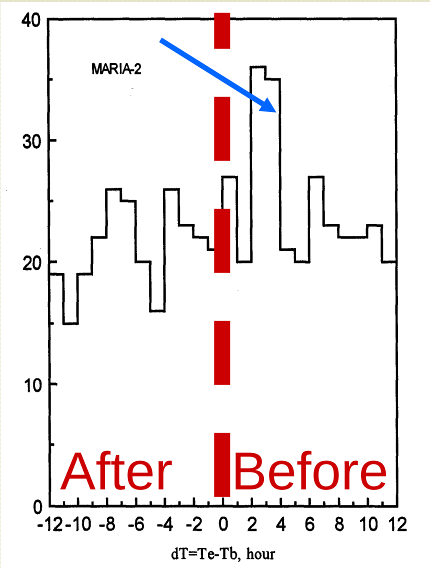


**MIR** mission
1985-2000

Altitude: 400 km

Inclination: 51°

**$E_e$: 20 ÷ 200 MeV**
**$E_p$: 20 ÷ 200 MeV**

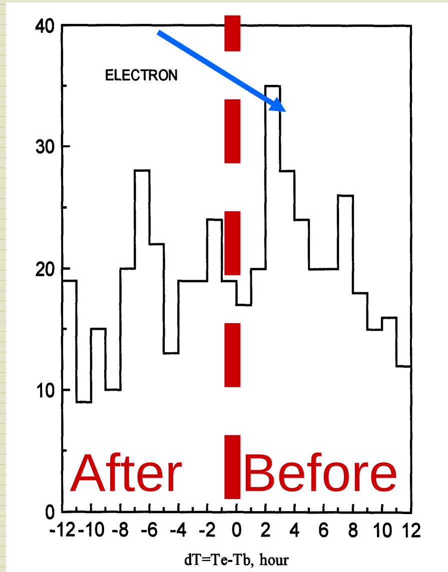


**METEOR-3** mission
1985-1986

Altitude: 1250 km

Inclination: 82°

**$E_e$: ≤ 30 MeV**

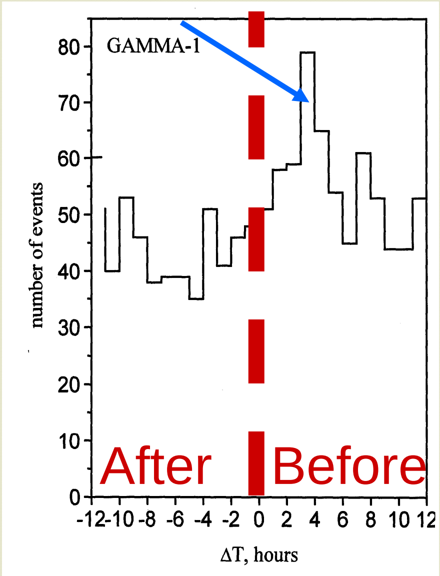


**GAMMA-1** mission
1990-1992

Altitude: 350km

Inclination: 51°

**$E_e$: > 50 MeV**

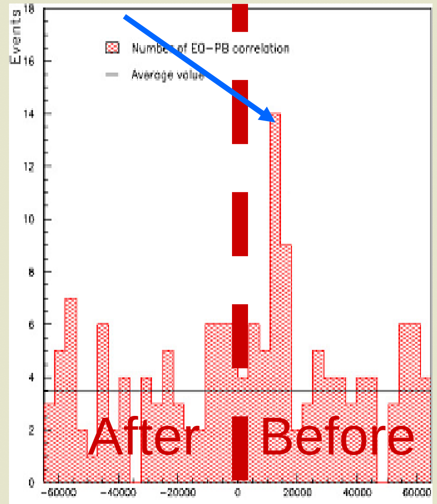


**ORR**
(Orbit Rate Rotation;
July 1992 - May 1994)

**SAMPEX/PET**
**Mission 1992-1999**

Altitude: 520÷740km

Inclination: 82°

**4 ≤ $E_e$ ≤ 15 MeV**

# Discussion & conclusions

- **PBs of precipitating high-energy Van Allen electrons appear to precede statistically by some hours the occurrence of moderate and strong EQs.**
- Several constrains and cuts have been applied to data in order to exclude correlation with non-seismic phenomena.
- **No correlation was found between PBs and other non-seismic sources.**
- The results we have obtained:
  - ✓give indication for a **deeper investigation of the physical mechanisms** under study
  - ✓ point out the **importance of satellite pointing modes**, **pitch angle reconstruction, high energy PDA, *detection of both electrons and protons* for longitude reconstruction, etc.**

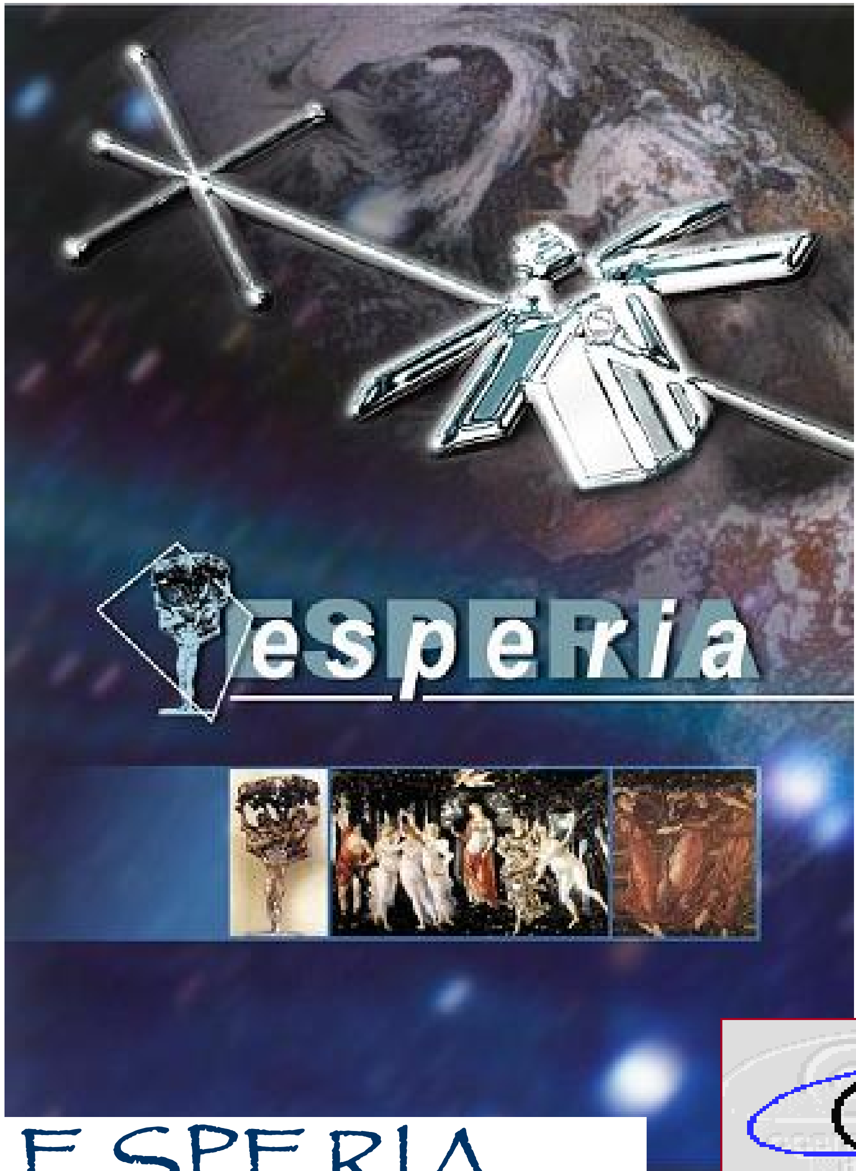


# ESPERIA project

agenzia spaziale italiana

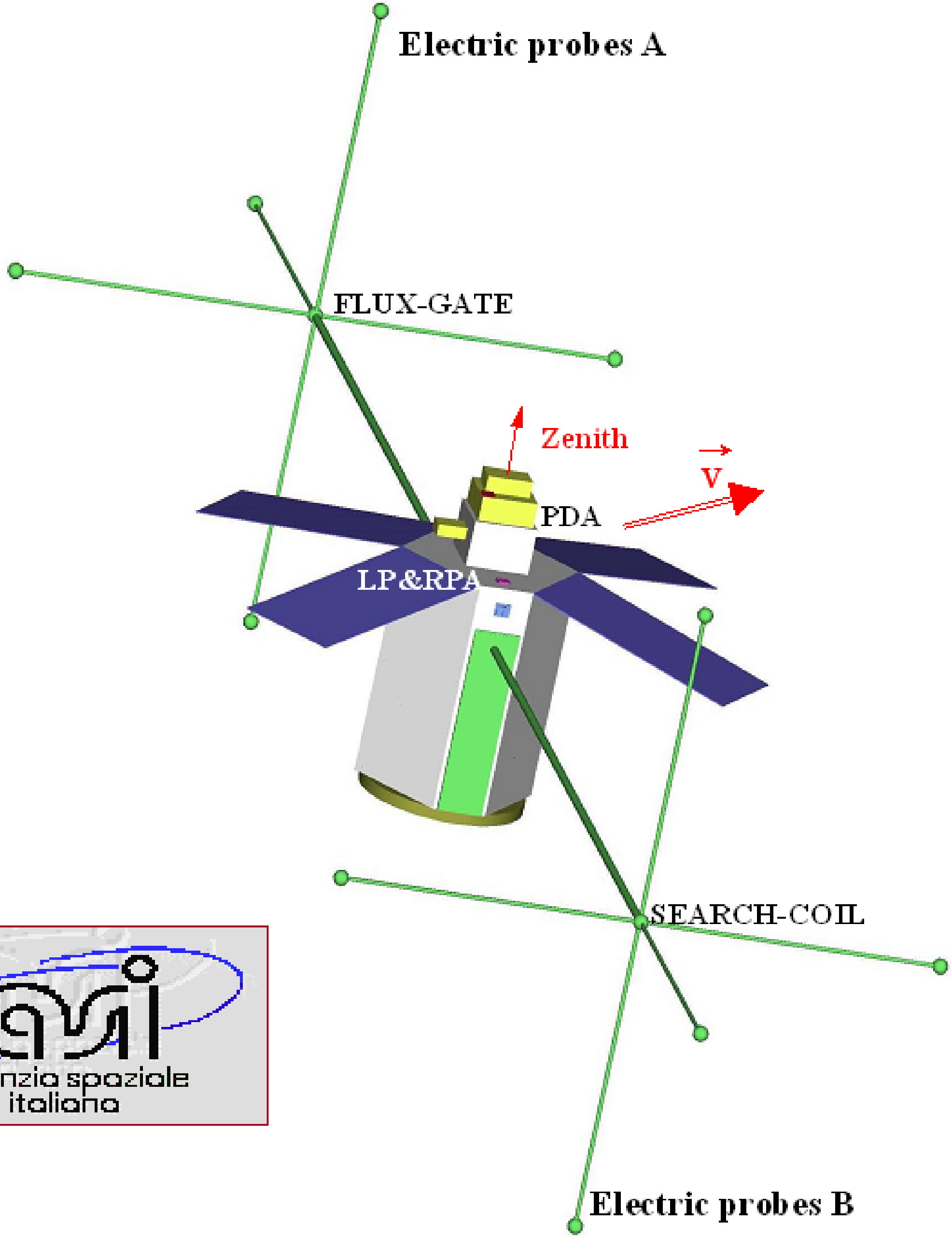

# L A Z I O

*"L'armi canto e 'l valor del grand'eroe
che pria da Troia, per destino a i liti
d'Italia e di Lavinio errando venne;
… e gli suoi dèi ripose in Lazio"*

*Virgilio, Eneide I, 1-9.*

UNIVERSITA' DEGLI STUDI DI ROMA Tor Vergata Università

ROMA TRE Università degli studi

INFN Istituto Nazionale di Fisica Nucleare

esa

S.E.R.M.S. s.r.l. Studio degli Effetti delle Radiazioni sui Materiali per lo Spazio

FILAS

G & A Engineering Microelectronics for Space

NERGAL

LAZIO

LOW
ALTITUDE
ZONE
IONIZATION
OBSERVATORY

&

ENEIDE mission

15-25 April 2005

Roberto Vittori

esa

EGLE

**E**speria
**G**eo-magnetometer
for a **L**ow-frequency
wave **E**xperiment

# LAZIO & EGLE

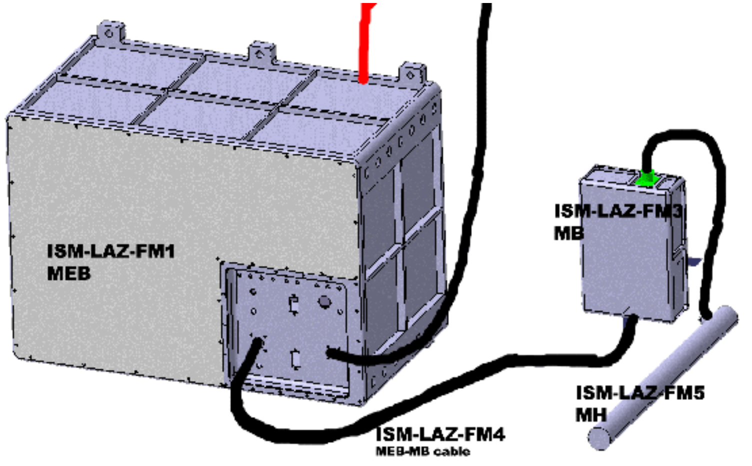
ISM-LAZ-FM1
MEB
ISM-LAZ-FM3
MB
ISM-LAZ-FM5
MH
ISM-LAZ-FM4
MEB-MB cable

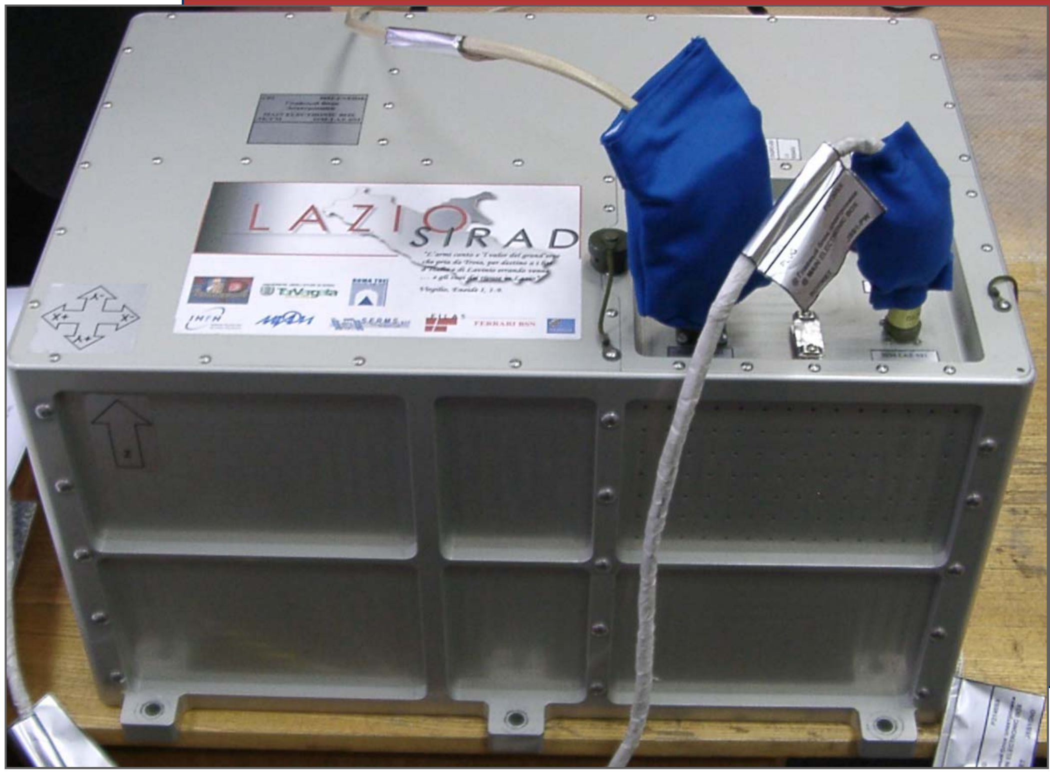
LAZIO
SIRAD


EGLE

# LAZIO-EGLE equipment

Main Electronic Box

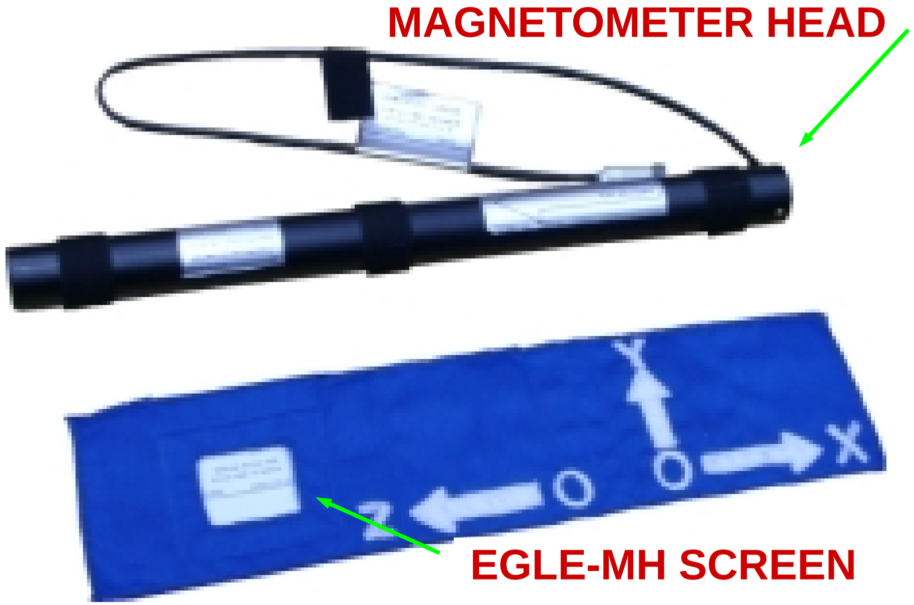



PCMCIA cards

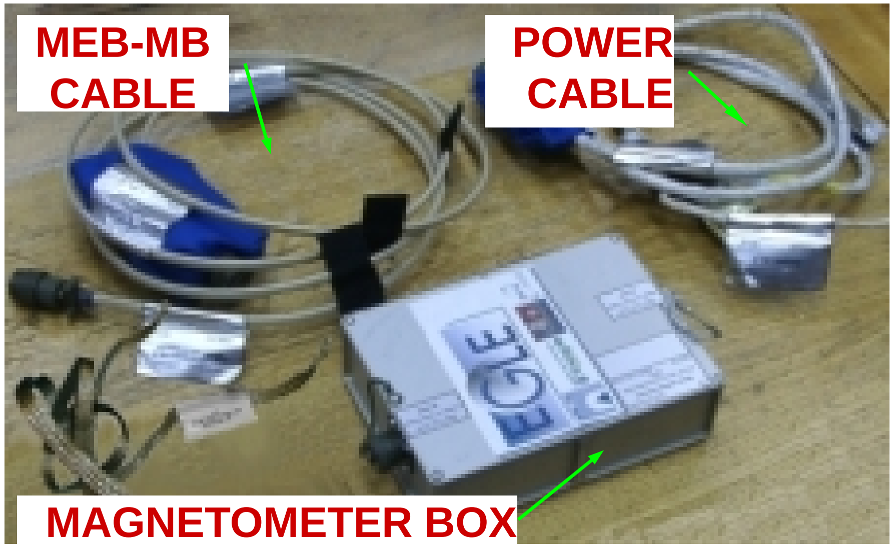

# L AZIO *P*article *D*etector *A*nalyser

## LAZIO particle detector

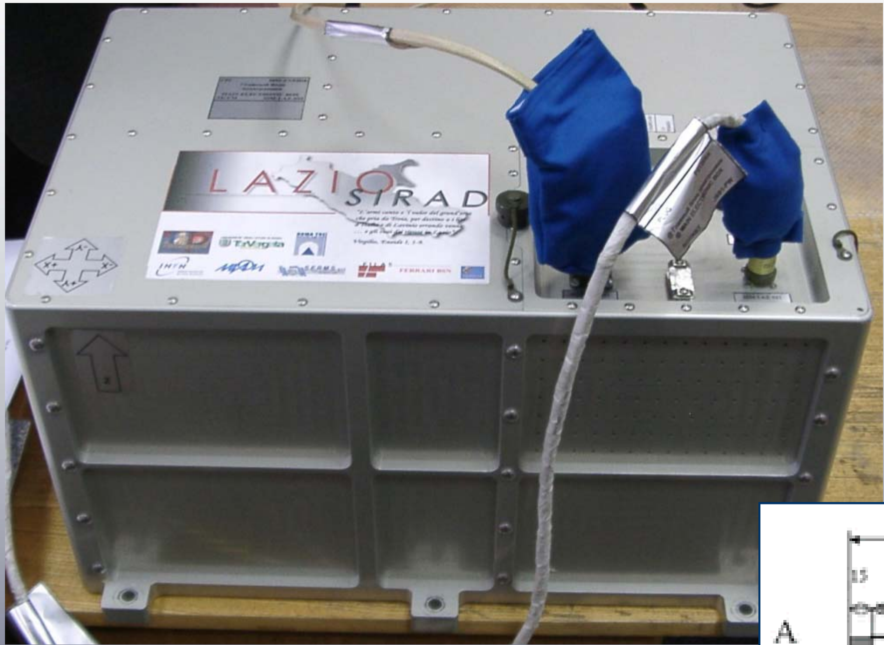

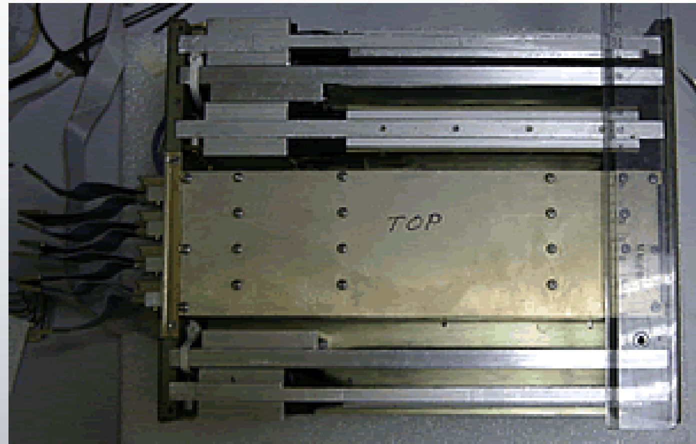

LAZIO scintillators layout

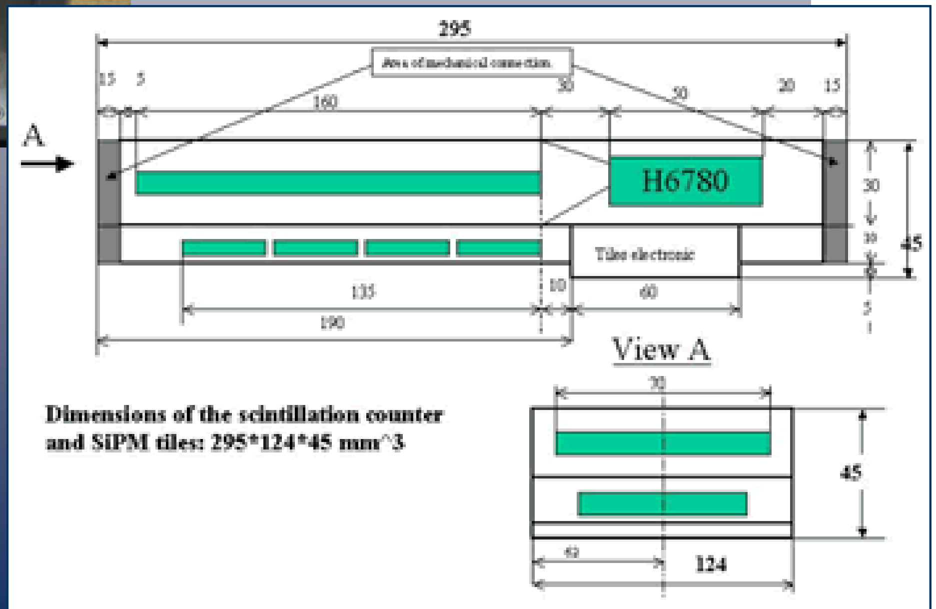

# EGLE includes a *single axis search-coil magnetometer MH*

Magnetic sensor (left),
EGLE acquisition board (bottom),
LAZIO–EGLE connection cable (top),
1–Wire–Serial board mounted on the pc tower (right).

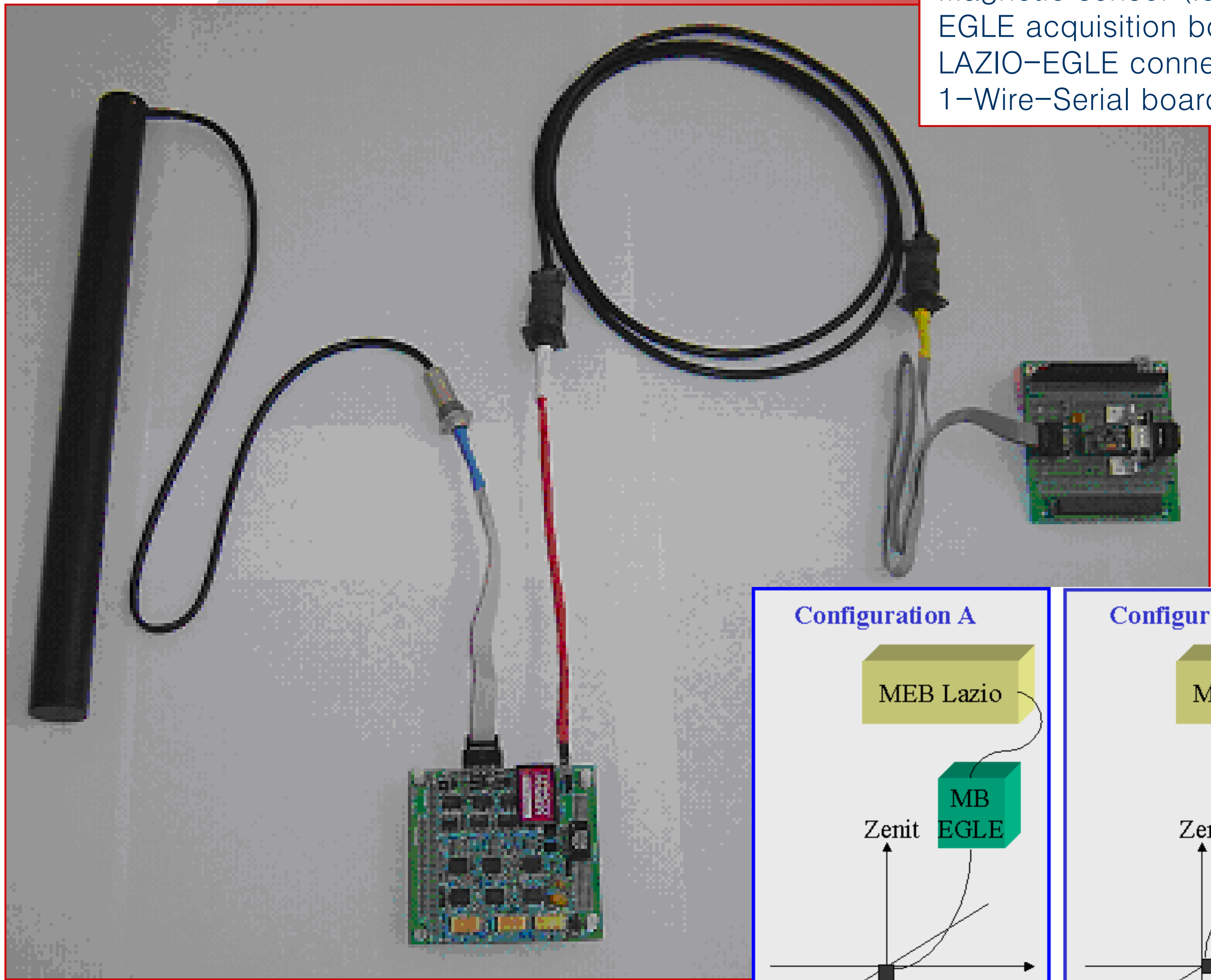

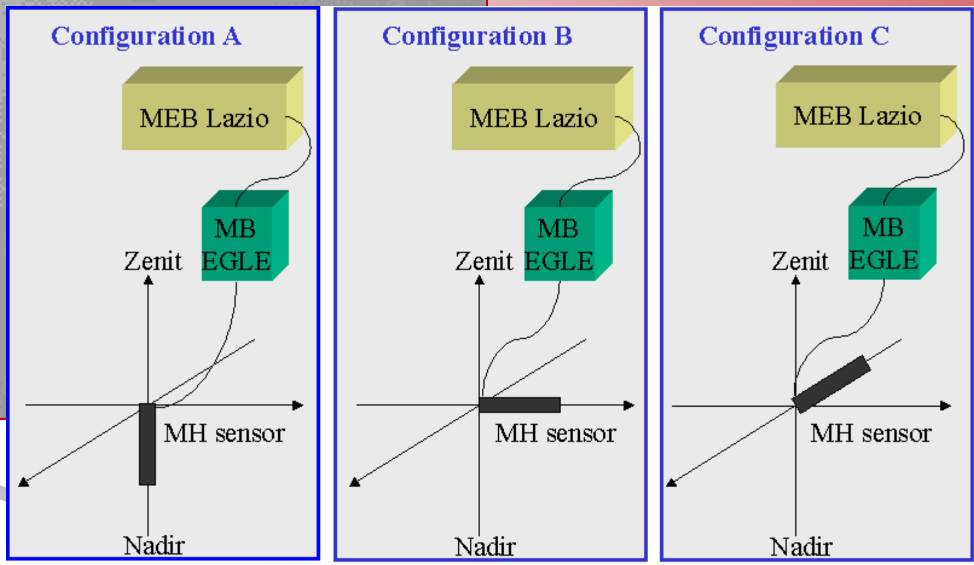

# EGLE magnetometer

| Basic technical specifications of the EGLE probe MH | |
|---|---|
| Frequency band of receiver signals | 0.5 ÷ 50000 Hz |
| Shape of transfer function | linear – flat |
| Type of output | Symmetrical |
| Transformation factor at both output terminals: | |
| • at linear part (0.5 – 5 Hz) | f*4 mV/(nT*Hz) |
| • at flat part (5 – 50000 Hz) | 20 mV/nT |
| Transformation factor error: | |
| ▪ at flat part of band pass without edges | ≤ ±0.25 dB |
| ▪ at flat part band pass edges | ≤ 3 dB |
| Magnetic noise level, $pT*Hz^{-1/2}$: | |
| ▪ at 5 Hz | ≤ 0.4 |
| ▪ at 100 Hz | ≤ 0.02 |
| ▪ at 5 kHz | ≤ 0.004 |
| ▪ at 50 kHz | ≤ 0.02 |
| Nominal output load | ≤ 200 pF<br>≥ 50 kΩ |
| Power supply voltage | ± (15 ± 0.2) V |
| Power consumption | 300 mW |
| Temperature range of operation | -30 °C ÷ +50 °C |
| Outer dimensions (without prominent parts) | l = 400 mm<br>d = 32 mm |
| Length of the output cable | 0.7 m |
| Weight | ≤ 320 g |

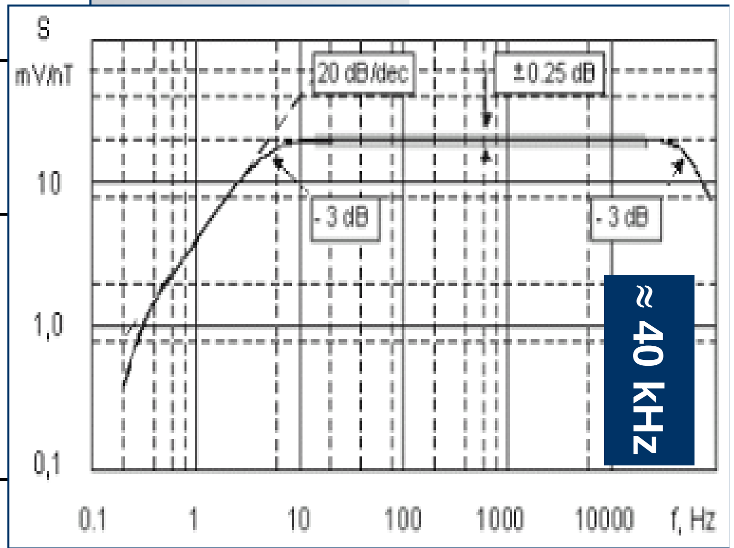


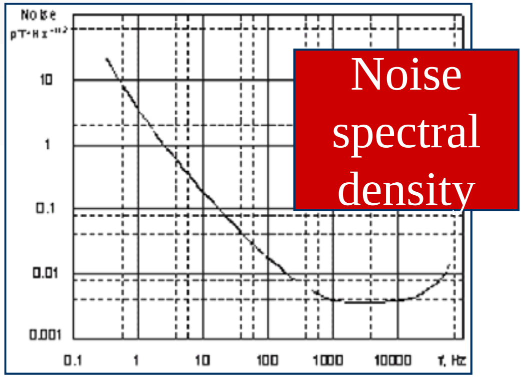

# EGLE

## **E**speria **G**eo-magnetometer for **L**ow frequency **E**xperiment


Search-coil frequency band : 0.5 Hz ÷ 50 kHz

| Channel | Frequency band | Type of data |
|---|---|---|
| **Channel A** | **$\leq$ 40 Hz** | Integrated r.m.s |
| **Channel B** | **(0.5 ÷ 5) kHz** | Integrated r.m.s |
| **Channel C** | **(20 ÷ 40) kHz** | Integrated r.m.s |
| **Channel D** | **$\leq$ 10 Hz** | Raw data |

*M*agnetic *f*ield

***ISS*** inclination 51.6º , altiyude ≈ 350-450 km.

# E gle Data Acquisition System

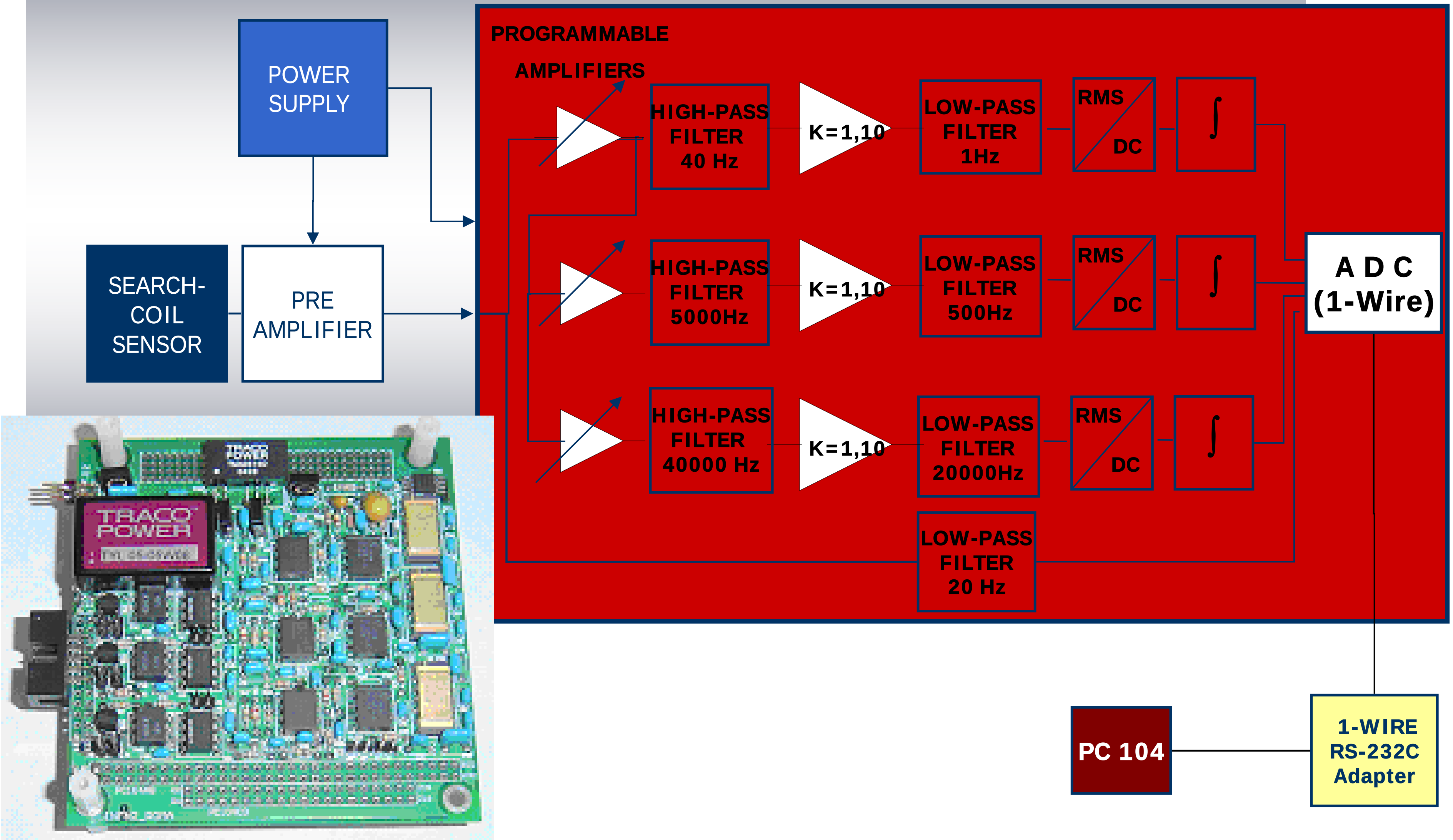

# Italian Soyuz *Eneide* Mission

## 15th April 2005

# LAZIO-EGLE Installation

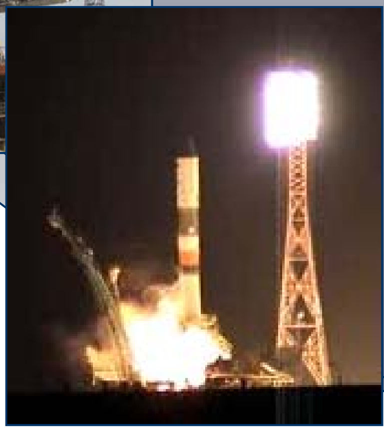

Soyuz 10S


Mis

# LAZIO

# EGLE

# LAZIO in the PIRS module

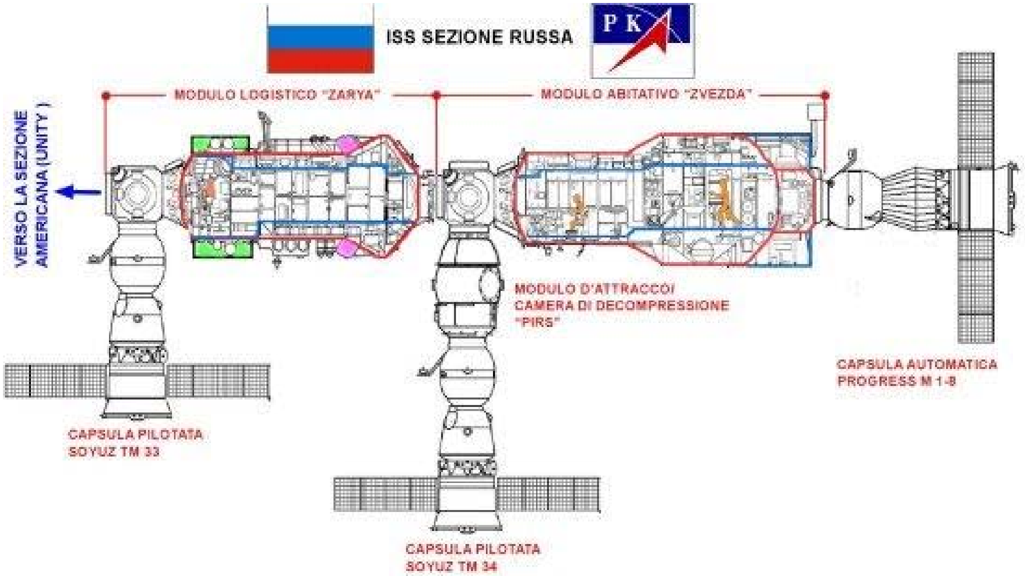


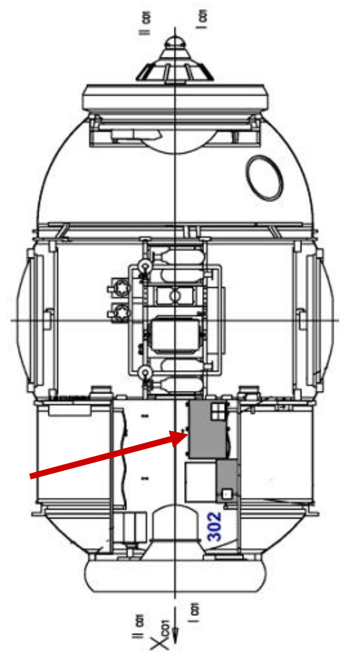


**Main Electronic Box**

## ENEIDE Mission 15-25 April 2005

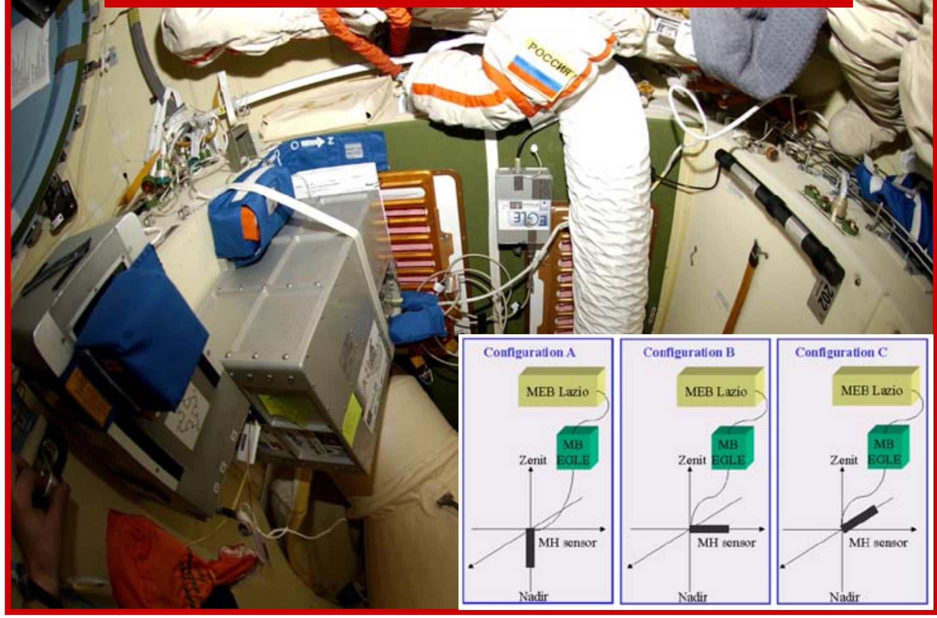


## Increment 14 (Autumn 2006-Spring 2007)

# *ENEIDE* mission

EGLE

***E**speria*
***G**eo-magnetometer*
*for a **L**ow-frequency*
*wave **E**xperiment*

**LAZIO**

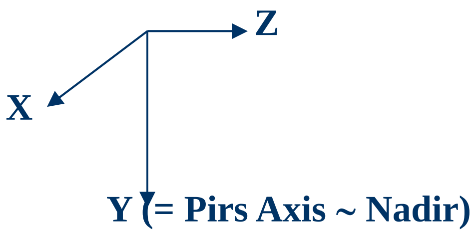

# Increment 14

October 3rd 2006

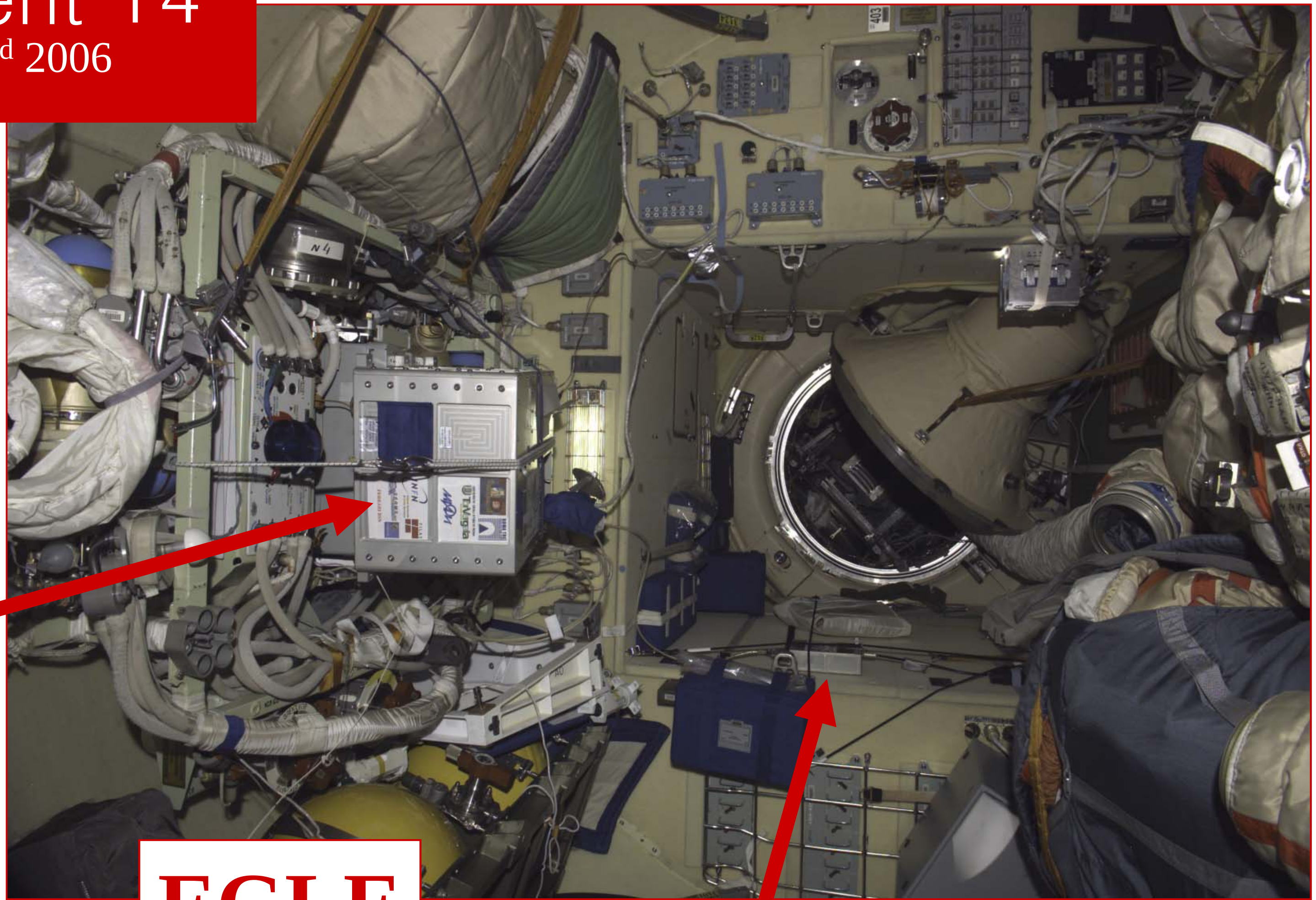

LAZIO

EGLE

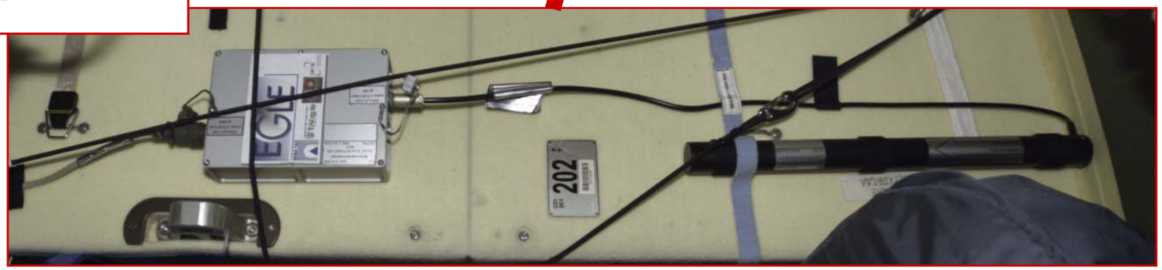

# Egle Channel C geographic map

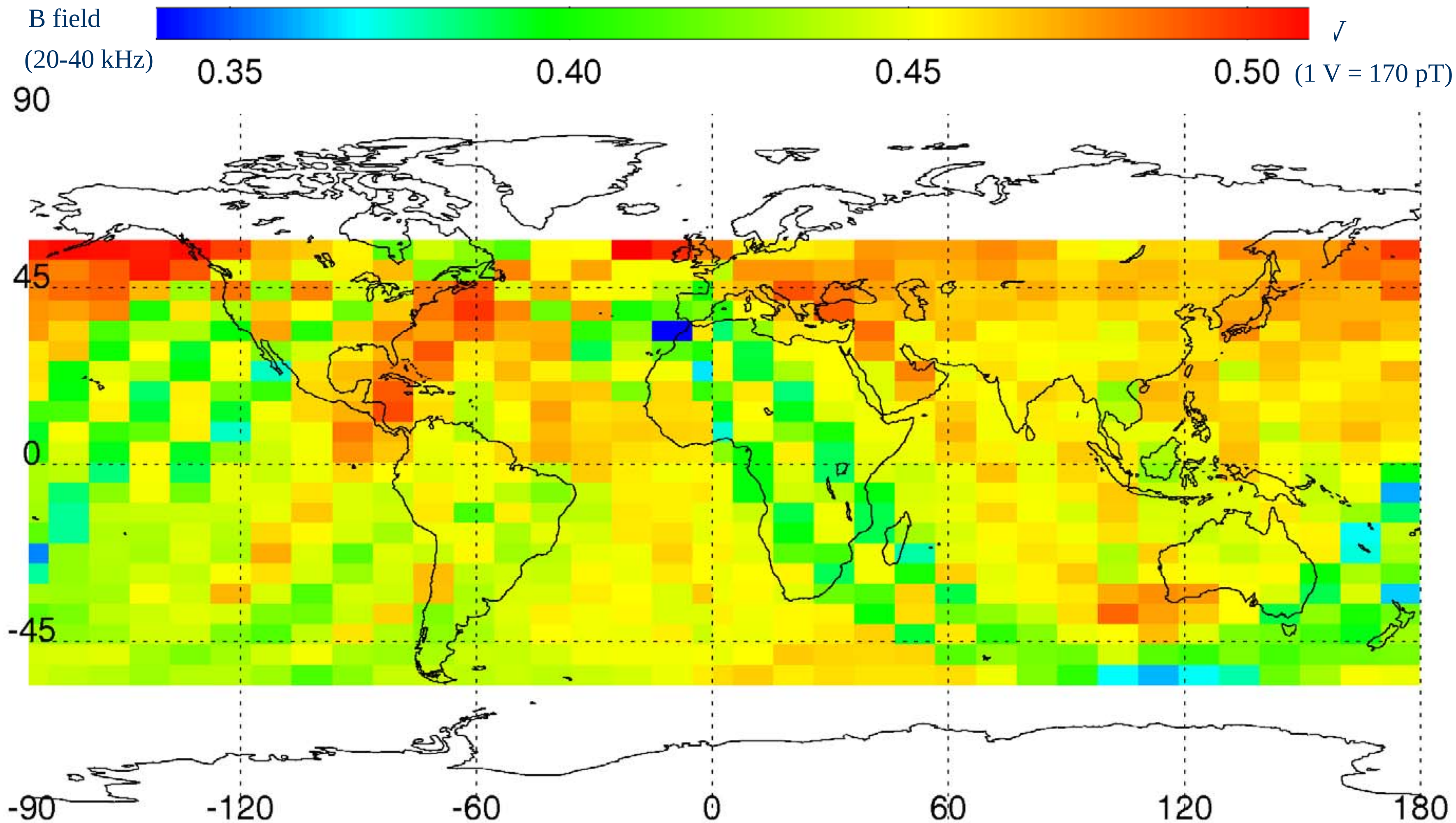


Sgrigna V. (*P.I.* EGLE), Buzzi A., Conti L., Stagni C., Zilpimiani D. – University Roma Tre, INFN, GAS

A
U
R
E
O
L

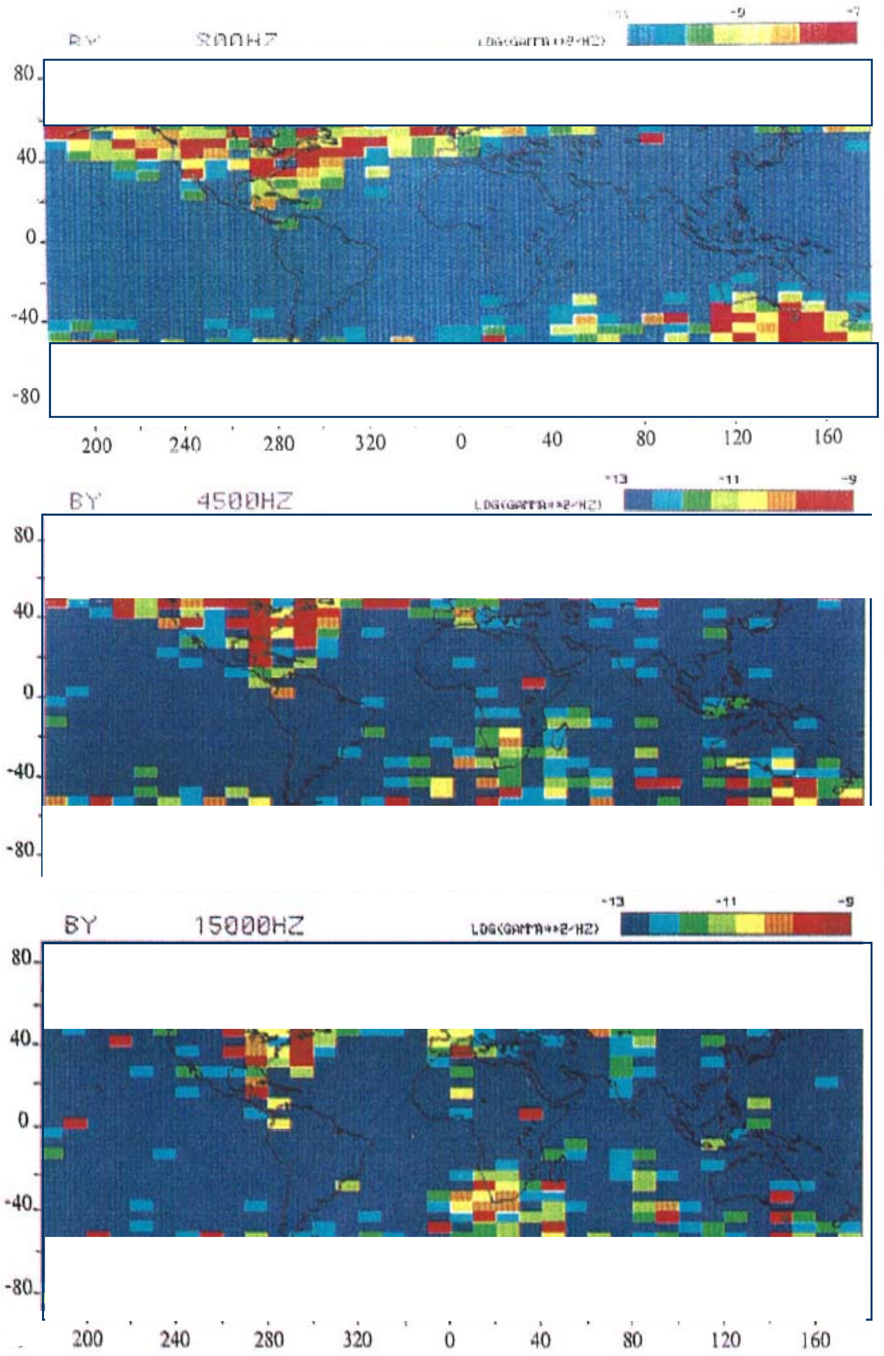

BY 4500HZ
BY 15000HZ
200 240 280 320 0 40 80 120 160


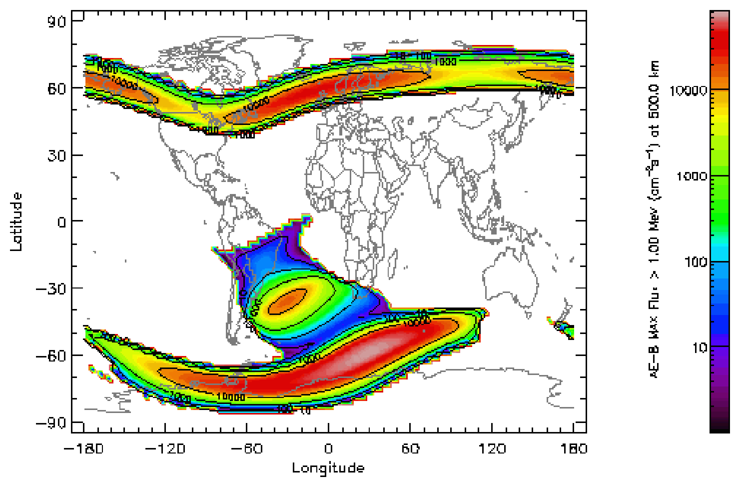

Latitude
Longitude


EGLE

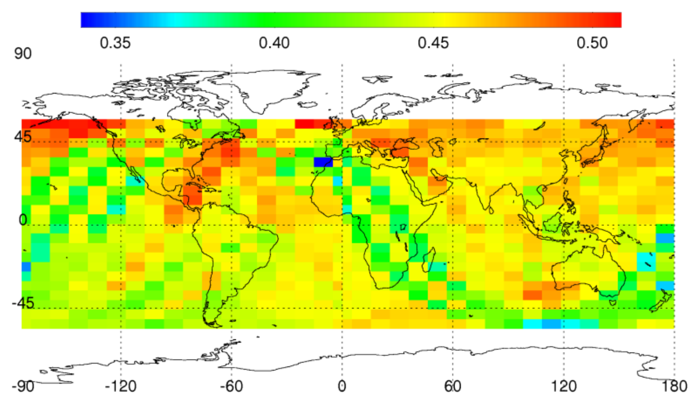

0.35 0.40 0.45 0.50
-120 -60 0 60 120 180

# EGLE magnetic field data

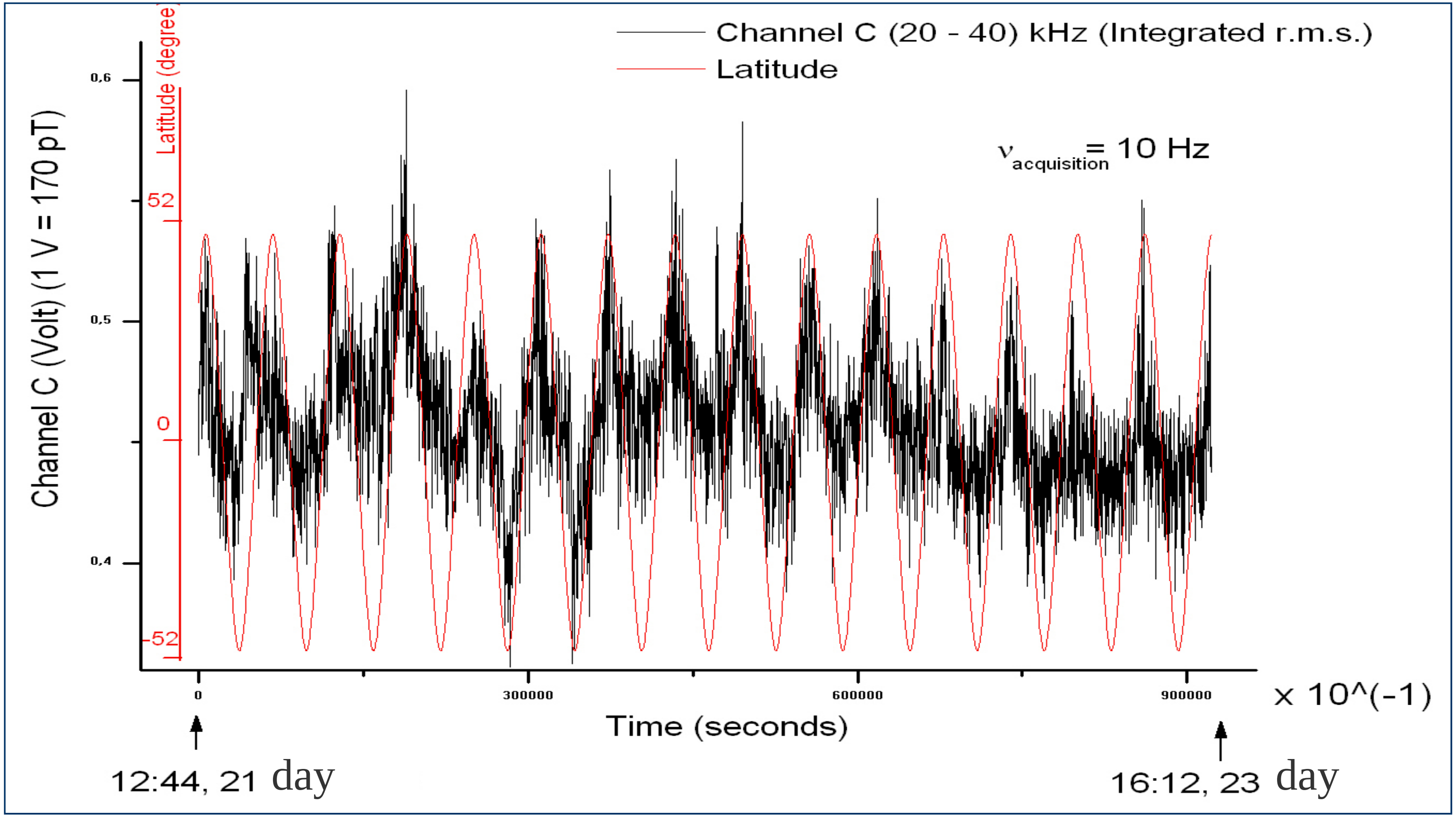

# Italian participants to the CSES collaboration

- **INFN** (Sections of Perugia, Rome, Trento, Bologna, Frascati)
- **ASI** – Italian Space Agency
- **Perugia University** (Perugia)
- **Trento University** (Trento)
- **“Tor Vergata” University** (Rome)
- **UNINETTUNO University** (Rome)
- **IFSI / INAF** (Rome)
- **CISAS** – ("G.Colombo", Padua)

# VOLTA Electric Field Detector (EFD) for the CSES satellite

- The EFD is constituted by **4 spherical sensors (probes)** coupled with the amplifying electronics and mounted on **4 deployable booms of 5 meter long each**.
- The continuous measurement of the **electric field vector components** from about DC / ULF up to HF (~15MHz) is obtained from the **measurement of the potential of the four probes which floats at the plasma potential**.
- Therefore, the electric field measurements will be affected by several effects such as: ***limitations of the electronics***, ***spacecraft electromagnetic noise***, ***different work functions of the probes***, and ***errors affecting the knowledge of position of each probe***.
- All the **hardware and the measurement procedures, suitable to reduce the electronic noise**, and to achieve the required dynamical range & resolution, will be adopted.
- The measurements along the three axes will be carried out in both the operating modes: **survey and burst** modes.
  - Particular care will be put in compensating effects due to variations of the S/C temperature.
  - Any effort will be done to keep errors (stemming from different work functions of the probes) below levels defined by the required dynamical range & resolution.

# VOLTA - EFD booms orientation

The spacecraft (S/C) is schematised as a cube of edge length 2L.
The x (parallel to the S/C velocity), z (points to nadir) and y axes, of the S/C reference system, have their origin at one of the cube's vertices.

**b is the length of each boom.**

S1, S2, S3, S4 are the positions of the four electric sensors in the S/C reference system. P1, P2, P3 and P4 are the fixation points of the booms on the S/C outer surface.

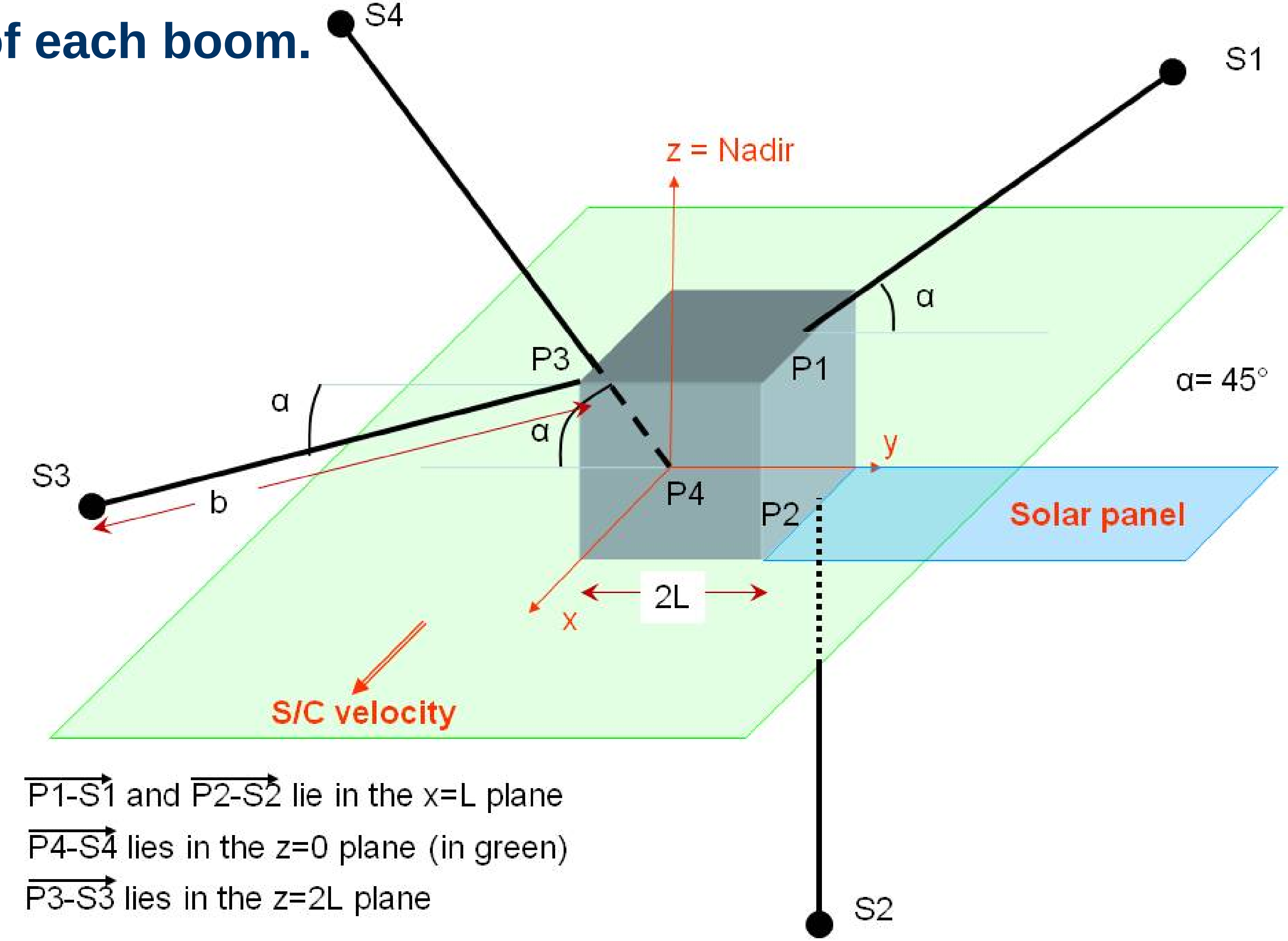

# Electric field resolution & booms stability

Errors affecting the **position of each probe** can stem from two different effects, which may present themselves at the same time:

✓ **variations the dipoles length** (with respect to their nominal value) due to booms oscillations (around their nominal direction),

&

✓ **misalignments of the x, y and z axes**.

A **constant deviation** of the booms, from their nominal position, would result in a **systematic error** (which would not concern us very much, if we look for variations of the quasi-DC field).

Conversely, **oscillations of the booms**, near their nominal position, have to banalysed with care, in order to understand what effect we should expect:

- **one or more lines** (at discrete and well-resolved frequencies) or
- **noise continuously covering a frequency band**.

# VOLTA - EFD booms

Figure shows the scheme of a deployed robotic boom.

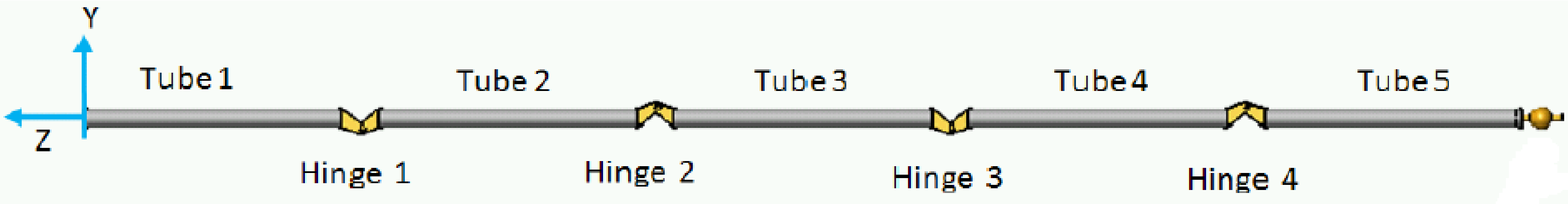


•The robotic booms ensure **high deployment reliability**, and **high stability** of their nominal position with respect to vibrations and misalignments.

•Moreover the robotic booms deployment mechanism **preserves the external booms coating** and allows to **protect cables** inside to the boom tubes.

•Consequently the robotic booms constitute one of the **best solutions** to be adopted for the EFD detector on the CSES satellite.

•Nevertheless, to **optimise volume** and **mass budget**, some alternative solutions, such as **collapsible hinge booms** and **Stacer booms**, are under evaluation by the CSES collaboration.

# VOLTA - EFD main specifications

| Frequency bands | Sampling frequency | Dynamic range |
|---|---|---|
| DC – 10 Hz | 100 Hz | ≥ 120 dB |
| 10 Hz – 2 kHz | ≥ 5 kHz | ≥ 90 dB |
| 2 kHz – 20 kHz | ≥ 50 kHz | ≥ 90 dB |
| 20 kHz – 3.5 MHz | ≥ 10 MHz | ≥ 70 dB |
| 3.5 kHz – 15 MHz | ≥ 40 MHz | ≥ 70 dB |

| | Total data rate (Gbits/day) |
|---|---|
| **ICE** | **~ 6** |
| **VOLTA** | **~ 42** |

| | |
|---|---|
| **Resolution** | 1 μV/m (DC – 10 Hz) |
| **Power supply voltage** | + 28 V |
| **Operating temperature (inside)** | -10 °C ÷ +45 °C |
| **Operating temperature (outside)** | - 30 °C ÷ + 60 °C |
| **Mass for each probe** | ≤ 0.5 kg |
| **Total Mass budget (including electronic box, but excluding booms)** | ≤ 10 kg |
| **Power consumption** | ~ 25 W (TBC) |
| **Data bus** | LVDS |
| **Operating mode** | Survey and Burst |

# VOLTA - EFD architecture

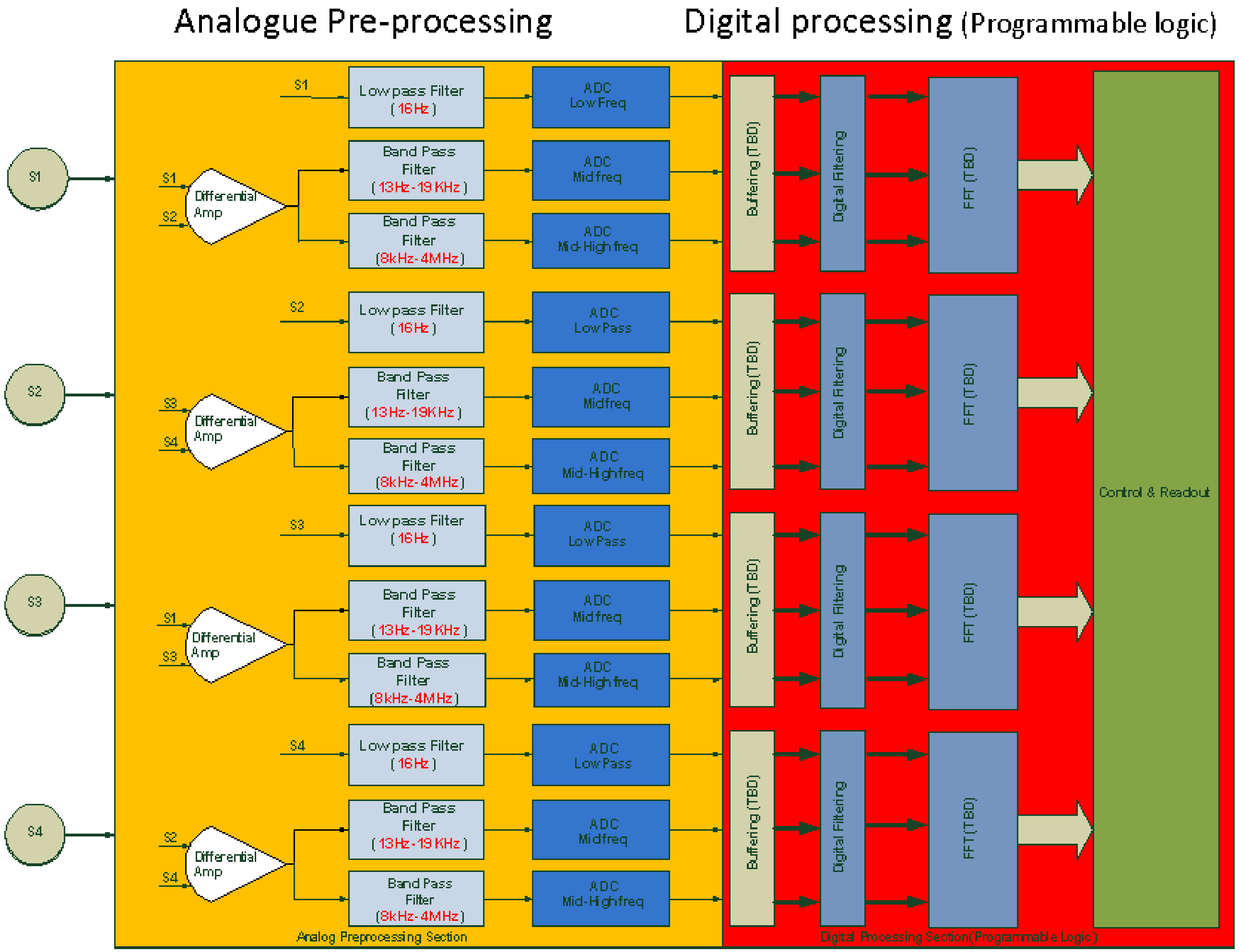


- **No analogue multiplexers are adopted** for selecting different inputs from sensors (4 DC-16 Hz potential waveforms will be always available) or from differential amplifiers providing different electric field waveforms above 13Hz (DEMETER adopted analogue multiplexer).
- This choice should ensure that **signals are cleaner and have a good S/N ratio**.

- Concerning the **analogue electronics** a simple **cold redundancy** will be adopted: if a section fails, it will be powered off and its redundant section will be powered on.
- Concerning the **digital electronics** we will adopt a **triple redundancy**.

# VOLTA - EFD probe: functional scheme

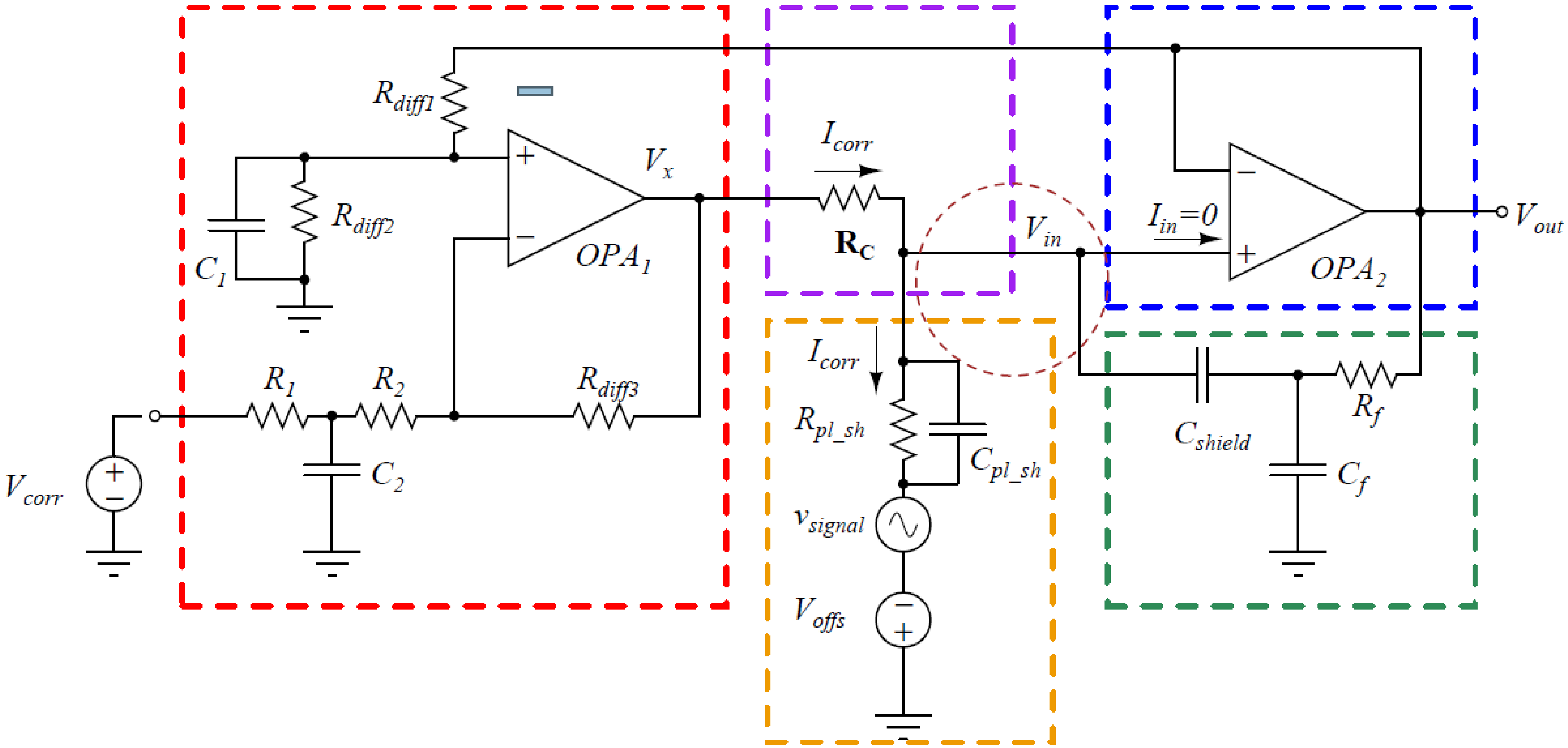


**Red box** (left) is the **circuit of the injection of current**.
**Purple box** (top - middle) is the **injection current correction**.
**Orange box** (bottom - center) represents the **plasma** model to be investigated.
**Blue Box** (top - right) is the voltage-follower circuit with high input impedance.
**Green box** (lower right) is the **filter on the intermediate screen**.
**The dashed circle in brown** represents the **sphere outside of the probe**.

# ICE – DEMETER vs VOLTA – CSES

- ✓ The preamplifier is installed on a small board inside a metallic box (ground shielding) located inside the spherical probe
- ✓ Operational amplifier is a low noise & high input impedance
- ✓ The EDF preamplifier board adopts several improvements with respect to the ICE-DEMETER solution constituted by: a reduction of the noise and tuning of some other parameters.

| | ICE – DEMETER | EFD – CSES satellite |
|---|---|---|
| OPA | OPA131 | OPA140 |
| *1/f noise* | 60 *n*V/Sqrt(Hz) @ 1*Hz* | 12 *n*V/Sqrt(Hz) @ 1*Hz* |
| *band width* | 4 MHz | 11 MHz |
| *Slew-rate* | 10 *V*/s | 20 *V*/s |

- ✓ Input resistance of about $10^{13}\,\Omega$, input capacitance of about pF.

# VOLTA- EDF Front-end electronics – Preliminary setup

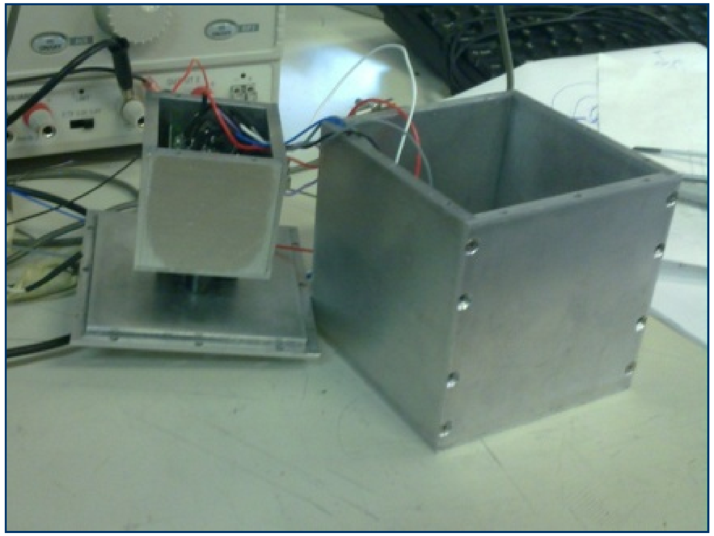

Two metal boxes emulate the probe and its internal shielding. The capacitance between them is 18 pF.

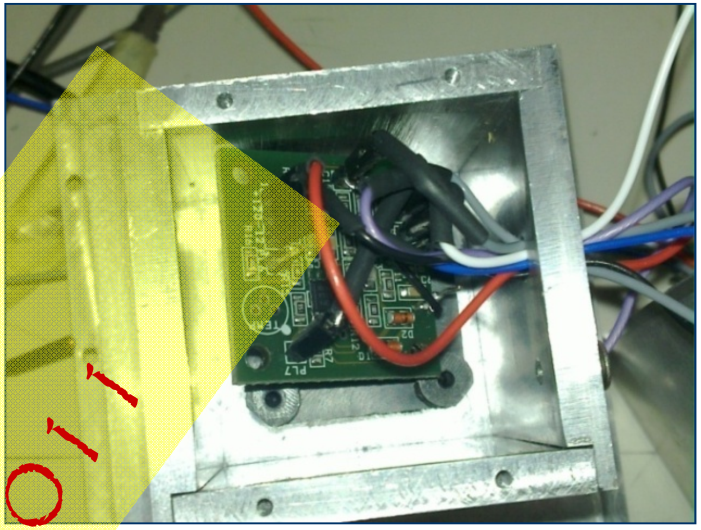

The box which emulates the probe has been placed in a shield connected to ground in order to isolate the probe from external noise. The capacitance between probe and grounded shield is 6 pF.

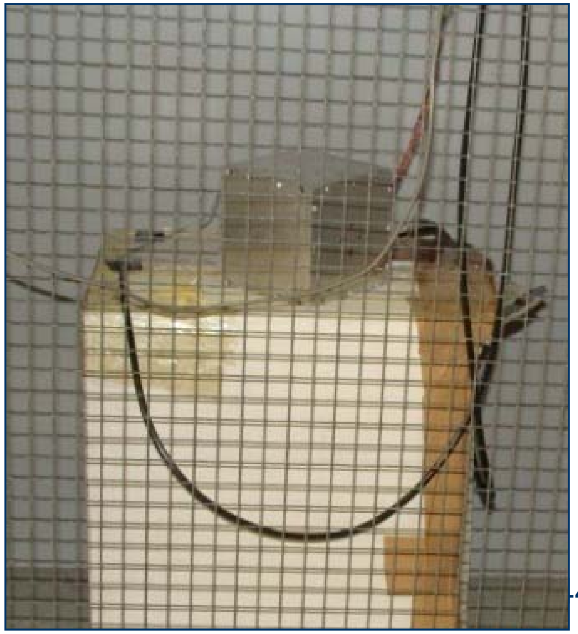

# VOLTA probe

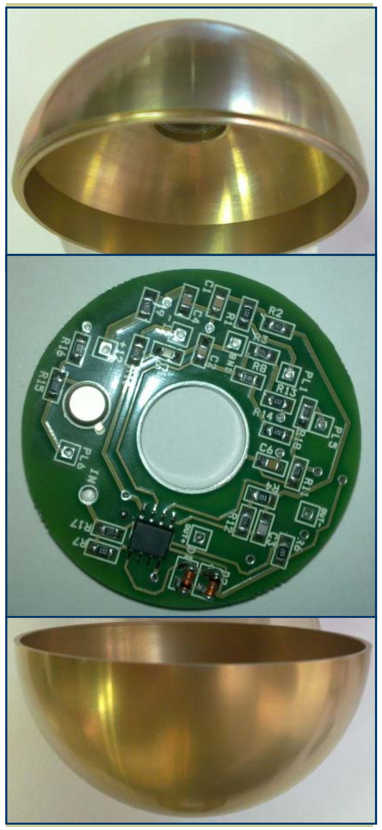

2012

VOLTA probe details

# VOLTA - EDF
# data acquisition
# &
# data handling board

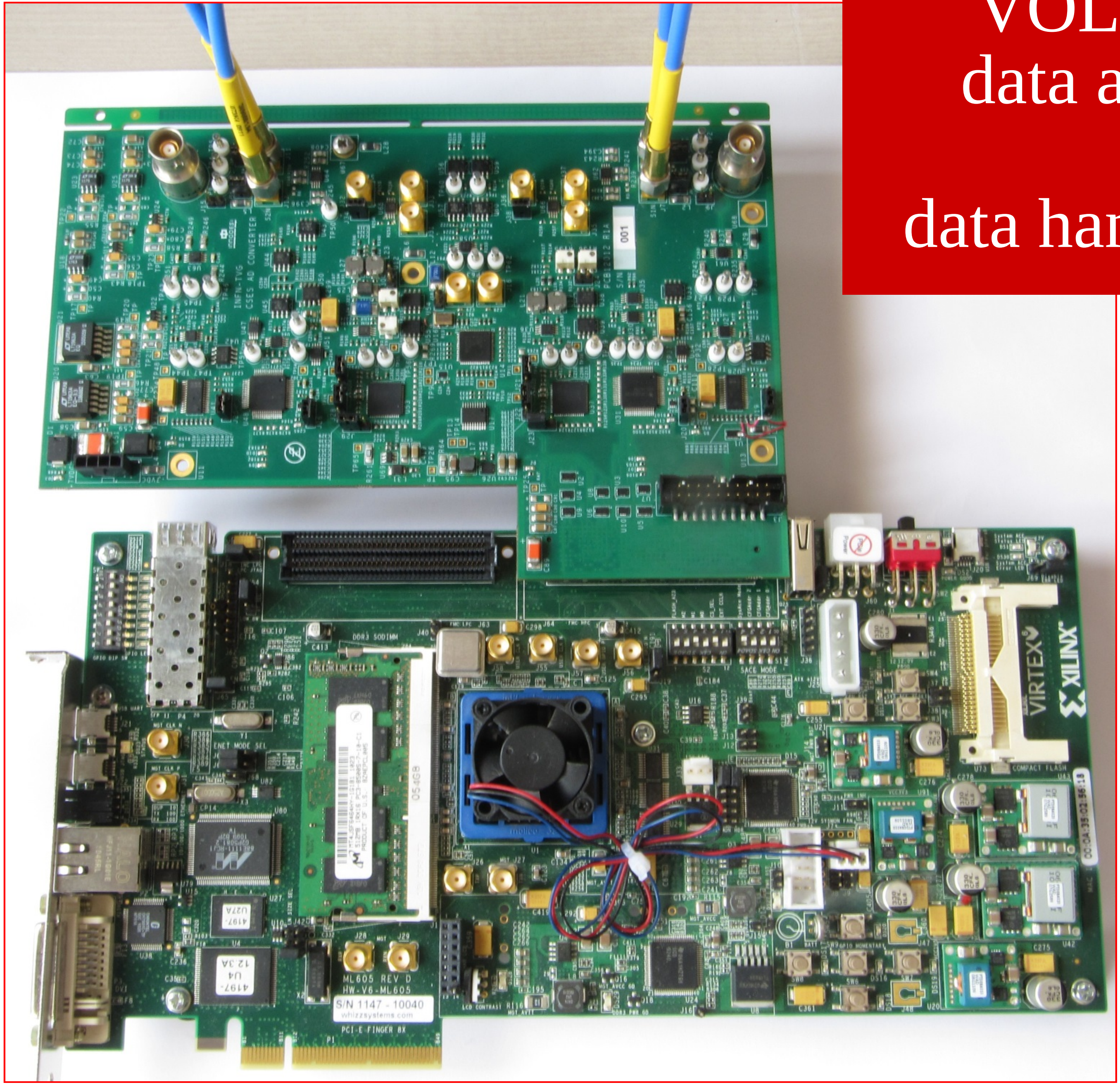

# Simulated Plasma characteristics

- Plasma impedance is a function of the plasma temperature and density conditions along the orbit.

- To take into account the variability of the plasma impedance, 3 different conditions have been considered: **configuration A** and **B** (with **extreme high density and temperature**) and the so called **configuration C** (**intermediate condition**).

| **Configuration** | n ($m^3$) | T (K) | R (Ω) | C (pF) |
|---|---|---|---|---|
| A | $10^{12}$ | 3000 | 67 | 29.0 |
| B | $10^{9}$ | 1000 | 970 | 4.8 |
| C | $10^{10}$ | 2000 | 660 | 6.6 |

# VOLTA - EDF probe test inside an anechoic chamber

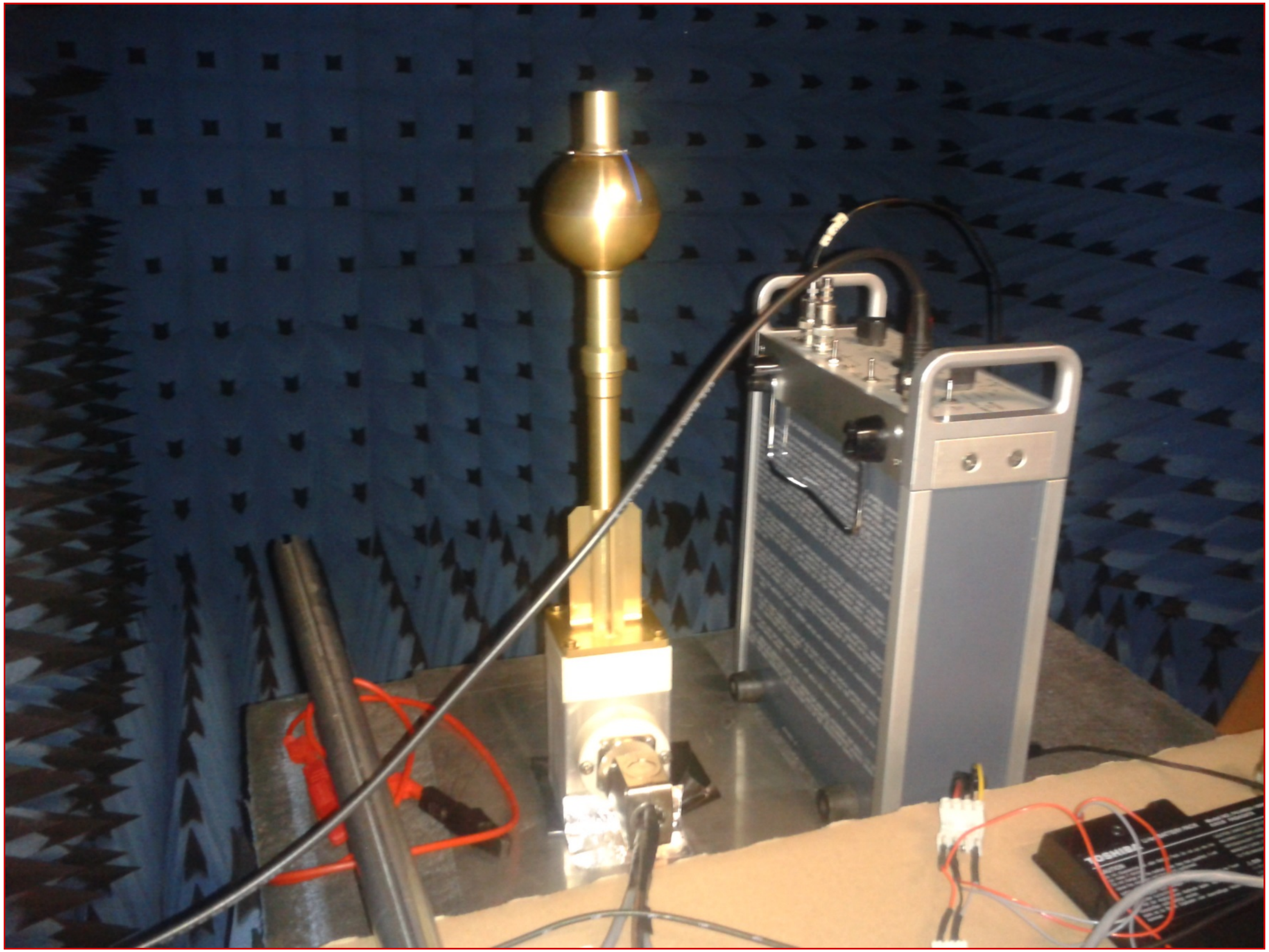

# VOLTA - EDF probe tested inside a Faraday chamber

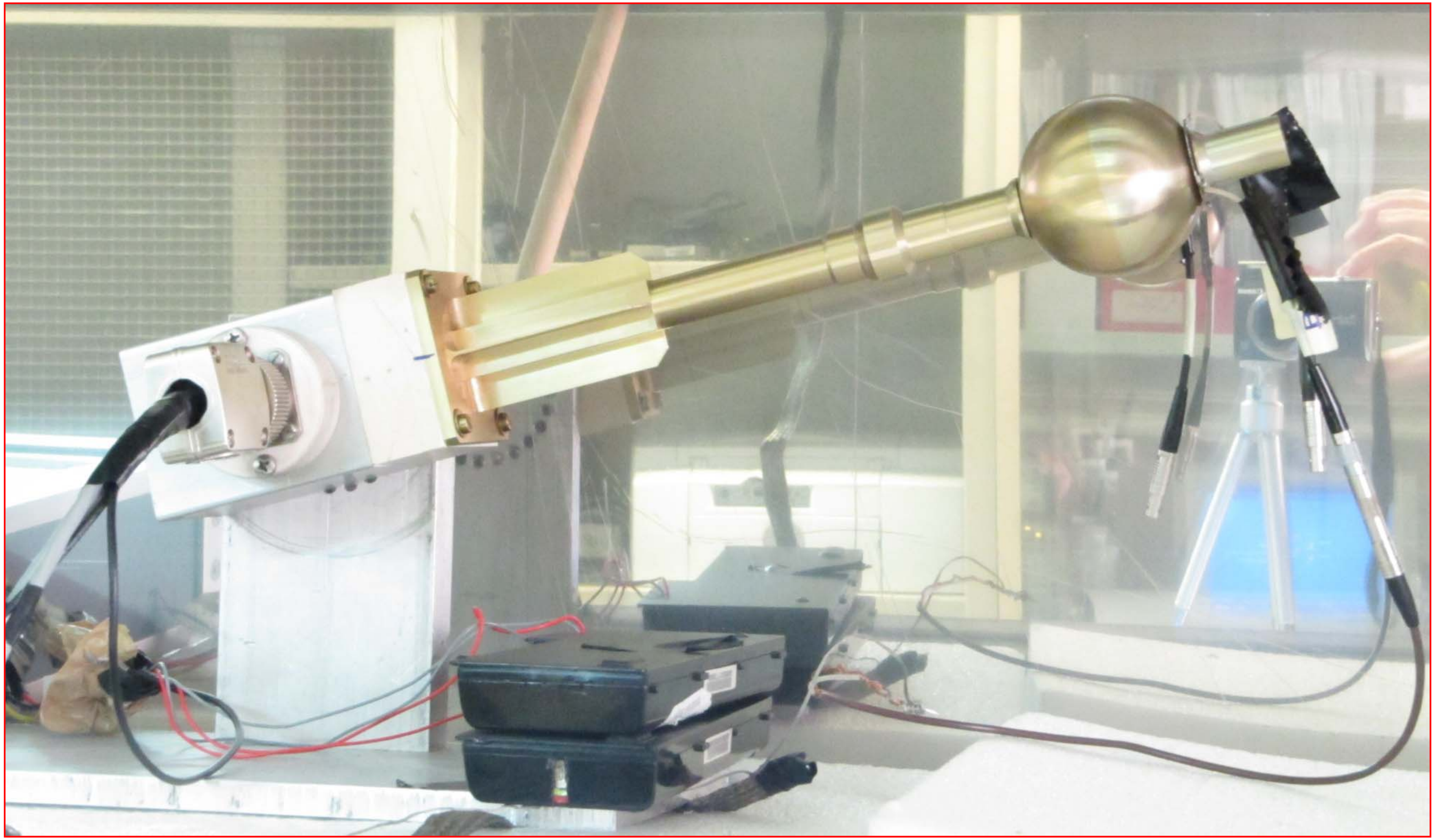

In order to test the front-end electronics under conditions similar to those which will be met in orbit, we consider 3 representative plasma conditions.

⇓

| Configuration | n (m³) | T (K) | R (Ω) | C (pF) |
|---|---|---|---|---|
| A | $10^{12}$ | 3000 | 67 | 29.0 |
| B | $10^{9}$ | 1000 | 970 | 4.8 |
| C | $10^{10}$ | 2000 | 660 | 6.6 |

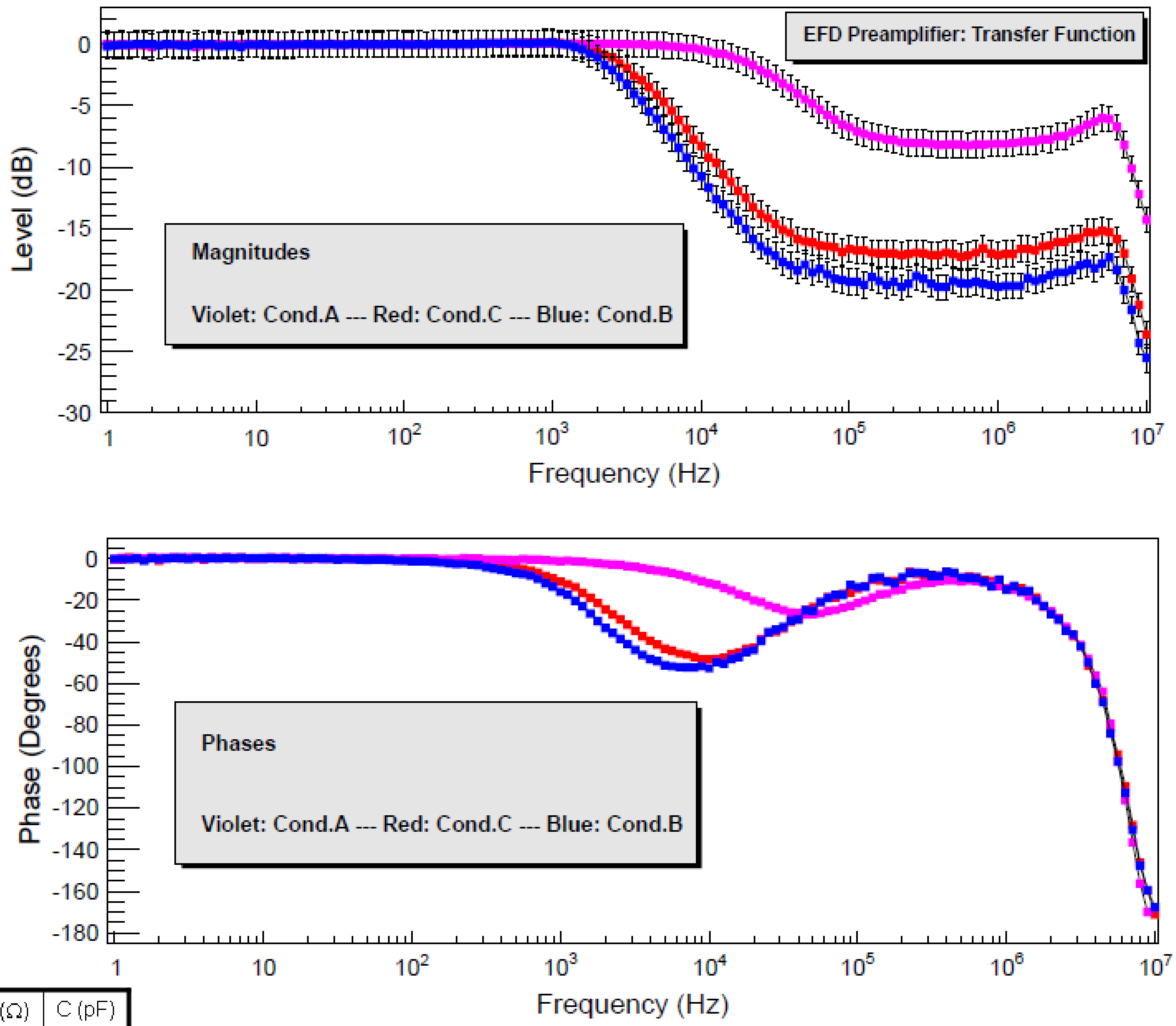

# EDF Preamplifier – Voltage Noise Density vs Frequency | BW (0-100kHz)

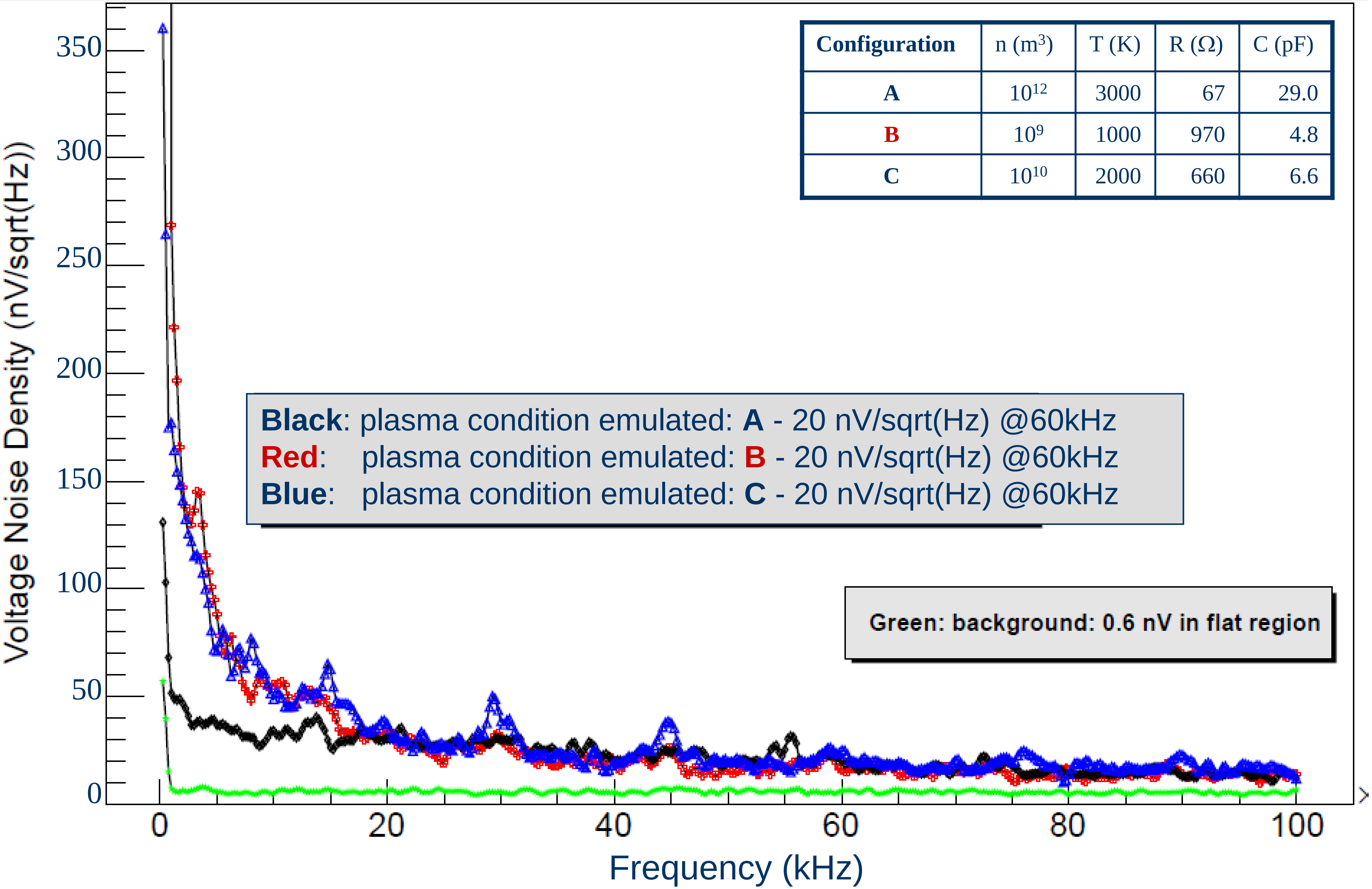


| Configuration | n ($m^3$) | T (K) | R (Ω) | C (pF) |
|---|---|---|---|---|
| **A** | $10^{12}$ | 3000 | 67 | 29.0 |
| **B** | $10^{9}$ | 1000 | 970 | 4.8 |
| **C** | $10^{10}$ | 2000 | 660 | 6.6 |

# EDF Preamplifier – Voltage Noise Density vs Frequency | BW (0.25-20Hz)

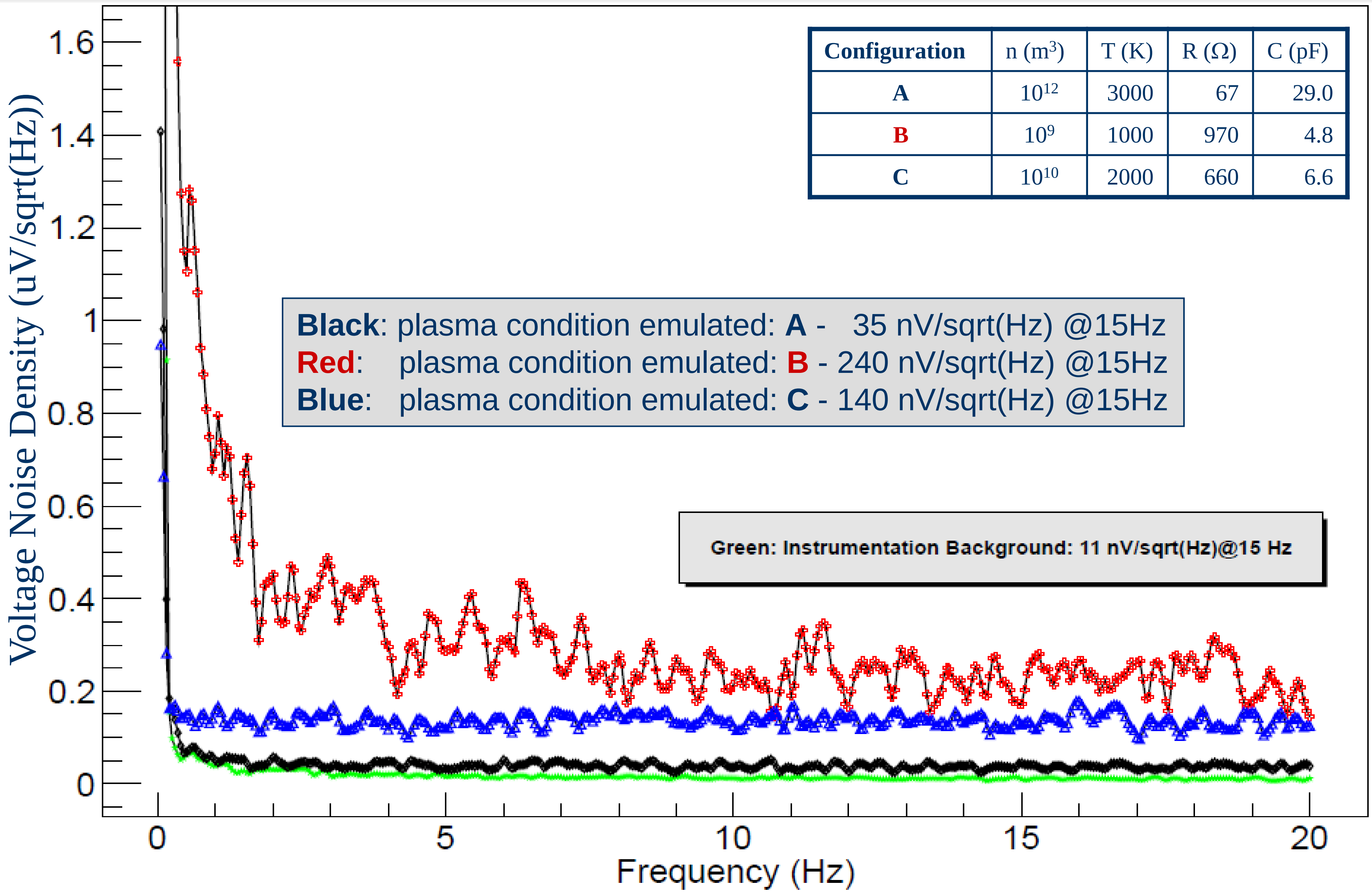


| Configuration | n ($m^3$) | T (K) | R (Ω) | C (pF) |
|---|---|---|---|---|
| A | $10^{12}$ | 3000 | 67 | 29.0 |
| B | $10^{9}$ | 1000 | 970 | 4.8 |
| C | $10^{10}$ | 2000 | 660 | 6.6 |

# VOLTA - EDF Transfer Function: at present

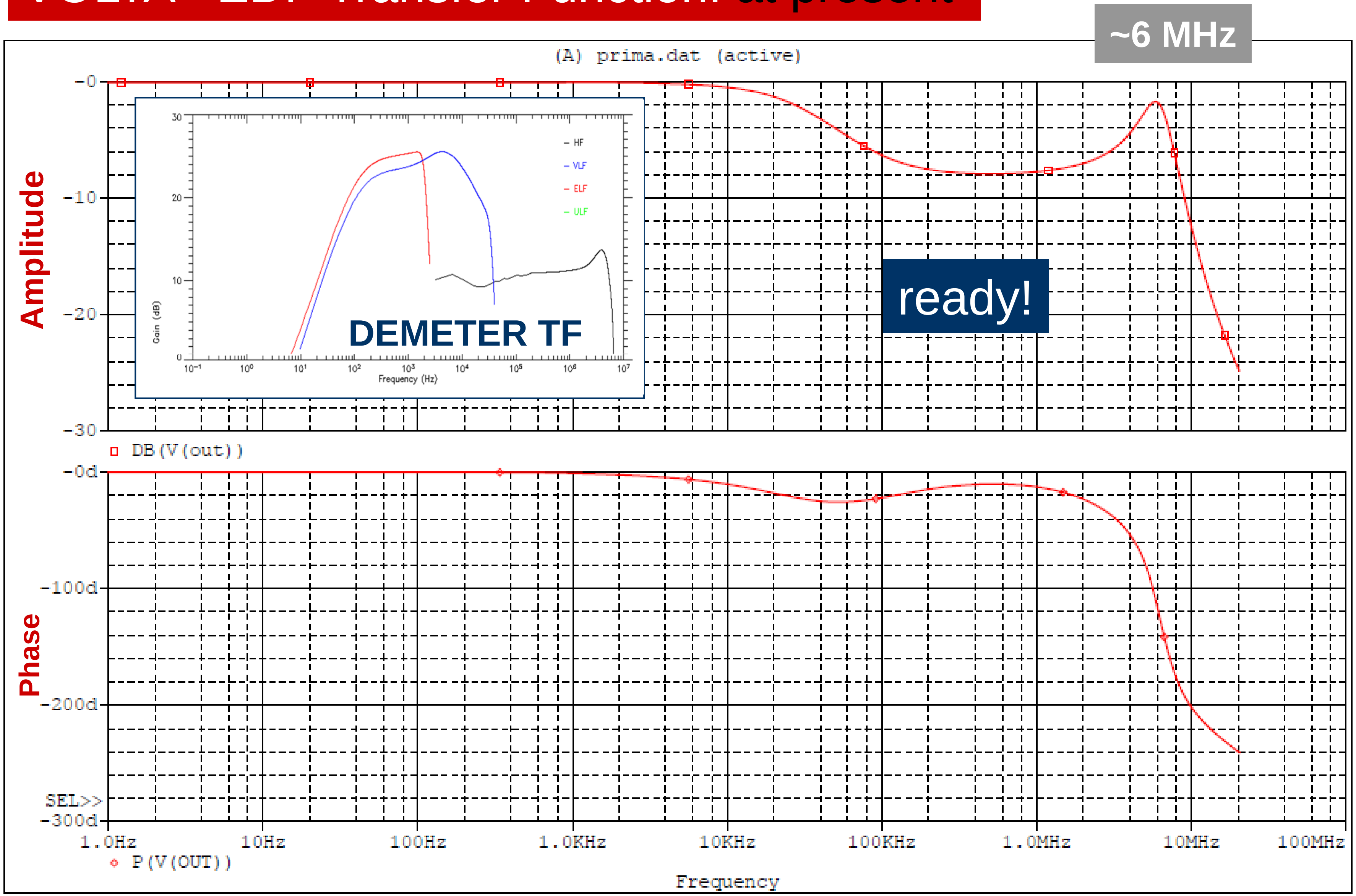

# VOLTA - EDF Transfer Function: the goal !!!

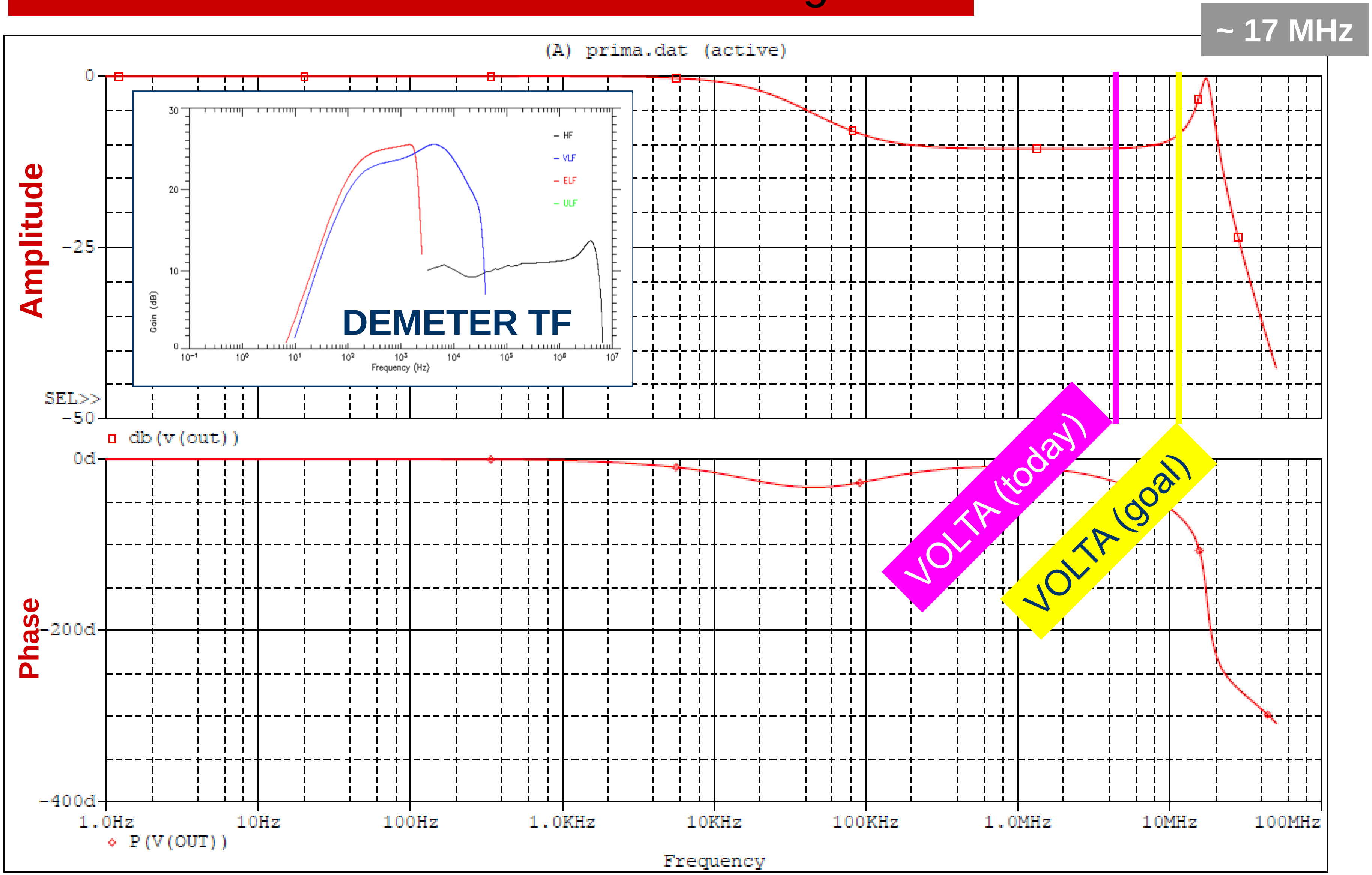

# OVER- preliminary

- **It has been added a differential output** to the pre-amplification system aimed **to increase the rejection of the common mode of the induced disturbances**.
- At this purpose it has been adopted the OPAMP THS4131 as single-ended-differential converter.
- **It whole system is under test** to evaluate the intrinsic and induced noise and **to verify advantages and disadvantages** of such a methodology.

thank you